**REVIEW ARTICLE**

# Gas-phase chemistry of molecular containers

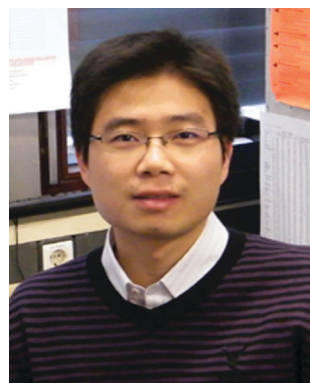Zhenhui Qi, Thomas Heinrich, Suresh Moorthy and Christoph A. Schalley*

The remarkable technical advances in mass spectrometry during the last decades, including soft ionisation techniques, the coupling of electrospray ionisation to flow reactors, and the broad scope of tandem mass spectrometric experiments applicable to mass-selected ions allow investigating the chemistry of molecular capsules in solution as well as in the absence of any environment. With these methods, mass spectrometry is capable of answering many questions starting from providing analytical characterisation data (elemental composition, stoichiometry, *etc.*) to structural aspects (connectivities, positions of building blocks in supramolecular complexes) and to the examination of solution and gas-phase reactivity including reactions inside molecular containers. The present article reviews this work with a focus rather on the chemical questions that can be answered than on the technical specialities of (tandem) mass spectrometry.

## 1 Introduction

Molecular containers[1] create void cavities inside their walls, in which molecules can be encapsulated that are then isolated from the bulk outside the container. Such encapsulation is reminiscent of natural binding pockets that occur in enzymes or ribosomes – in particular when the molecular container is based on non-covalent bonding and can reversibly open and close. Fabricating synthetic molecular containers is a way to affect the guest molecule in a highly controlled and specific manner and to change its reactivity significantly by providing a particular environment to it.[2] Since Breslow's pioneering work on cyclodextrins as enzyme mimics,[3] the design of synthetic

*Institut für Chemie und Biochemie, Freie Universität Berlin, Takustraße 3, 14195 Berlin, Germany. E-mail: christoph@schalley-lab.de; Fax: +49 30 838 55367; Tel: +49 30 838 52639*

molecular containers has progressed in an amazing way making use of calixarenes and resorcinarenes,[4] cucurbiturils,[5] carcerands,[6] and other scaffolds.[7] Among supramolecular containers, those based on hydrogen bonding[1,8] and metal coordination[9] are the most prominent and meanwhile provide quite huge interior spaces. For example, Fujita's metallo-supramolecular $M_{24}L_{48}$ containers[10] are made from 72 components (48 identical ligands on the edges and 24 metal ions at the vertices of a rhombicuboctahedron) and its molecular weight exceeds 20 kDa. Similarly, the hydrogen-bonded resorcinarene and pyrogallarene hexamers reported by Atwood[11] and Mattay[12] comprise an inner volume of *ca.* 1200 Å$^3$. Another interesting aspect of supramolecular containers is their reversible formation. Encapsulation in these capsules therefore creates a mechanical barrier for guest encapsulation and release.[13] As non-covalent bonds are sensitive to effects of the environment and potentially also to chemical stimuli added to the capsules, options exist to fine-tune the

*Zhenhui Qi received his Master degree under the supervision of Prof. Junqiu Liu and Prof. Jiacong Shen from Jilin University, China in 2009. Then, he obtained his PhD degree at Freie Universität Berlin, Germany, in the group of Prof. Dr Christoph A. Schalley. His research interests focus on mass spectrometry, responsive materials, and functional surfaces.*

**Zhenhui Qi**
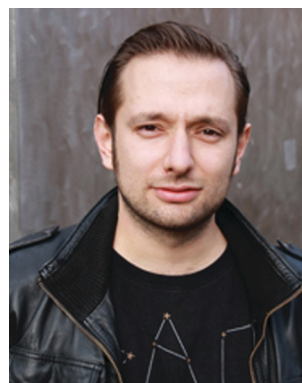
*Thomas Heinrich studied chemistry at Freie Universität Berlin. He obtained his Bachelor degree under the guidance of Rainer Haag and his Master degree in the group of Christoph A. Schalley. Since March 2013 he has been carrying out his doctoral research work in the same group. His research focuses mainly on Supramolecular Chemistry at interfaces where he develops switchable surfaces with the aim of establishing molecular machines.*

**Thomas Heinrich**

This journal is © The Royal Society of Chemistry 2015

*Chem. Soc. Rev.*, 2015, **44**, 515–531 | 515

gating processes and thus to control encapsulation and to alter guest reactivity inside catalytically active containers.[14]

With containers at hand that grow in size as well as their complexity, their characterisation becomes increasingly challenging. For a convincing characterisation, a number of different complementary methods need to be applied. While X-ray crystallography and NMR spectroscopy are currently and will likely continue to be the two most commonly employed analytical methods, mass spectrometry has seen a quite vivid development recently and is now a very valuable technique for the characterisation of supramolecules[15] providing the three "S" advantages outlined by McLafferty: specificity, sensitivity and speed.[16] The intact ionisation of complete viruses – such as the tobacco mosaic virus with its more than 2100 non-covalently bound protein subunits surrounding a templating RNA strand[17] – and intact virus capsids – such as the hepatitis B virus capsids[18] – clearly shows how far the limits of the characterisation of molecular capsules by mass spectrometry can be pushed forward.

Beyond analytical characterisation, mass spectrometry also serves for the analysis of solution processes. In particular, electrospray ionisation can be directly coupled to liquid chromatography as well as mixed-flow devices[19] or even micro-fluidics[20] (Fig. 1). Studies of both, biological and chemical processes,[21] such as protein folding,[22] enzyme catalysis,[23] the identification of reaction intermediates[24] and of error correction processes in self-assembly[19] illustrate the potential of mass spectrometry for monitoring processes occurring in solution.

On the other hand, mass spectrometry is a method for the investigation of completely desolvated ions in the high vacuum. The absence of any environment provides access to the ions' intrinsic properties which differ significantly as compared to their properties in condensed phase. This is particularly true for non-covalent complexes. In addition, reactivity studies on
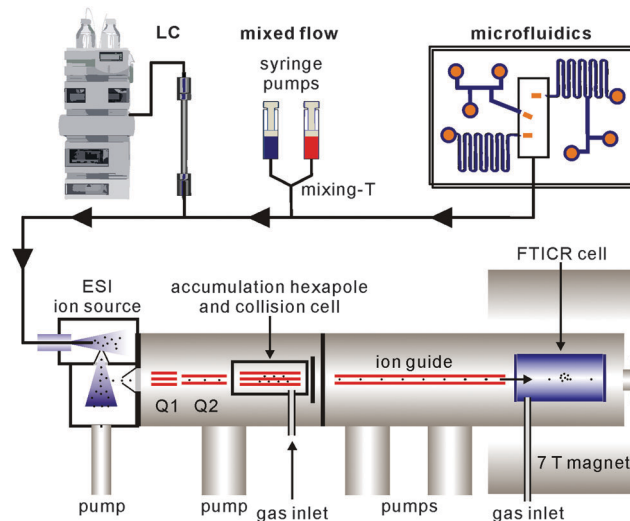


Fig. 1 Schematic illustration of various devices that can be interfaced with ESI-MS: liquid chromatography (left), mixed-flow reactors (centre) and micro-fluidic devices (right). We show here the coupling to an electrospray ionisation Fourier-transform ion-cyclotron-resonance (ESI-FTICR) mass spectrometer. Coupling to other types of ESI instruments is similarly possible.

isolated ions in the gas phase occur under conditions which do not allow the dynamic exchange processes between the supramolecules. While one, for example, observes fast guest and building block exchanges in solution, reactivity studies in the gas phase rather reveal intramolecular rearrangements and therefore provide a very different view on reactivity.

Modern mass spectrometers provide a number of different tandem MS experiments that can be used to investigate the structure and reactivity of a desired ion in the gas phase. The prerequisite is a mass-selection step prior to the gas-phase experiment (Fig. 2, top). Different types of mass spectrometers perform this mass-selection differently. The figure shows a quadrupole as

**Suresh Moorthy**

*Suresh Moorthy received both, the Bachelor and Master of Science in Chemistry from Bharathidasan University, Trichy, India. He obtained his PhD from Central Salt and Marine Chemicals Institute, Bhavnagar, India in the area of Supramolecular Chemistry under the direction of Dr Amitava Das. He spent one year Humboldt postdoc Fellowship at Freie Universität Berlin, Germany, with Chris Schalley in 2013. He is currently doing his postdoc at the University of Queensland, Brisbane, Australia. His research interest focuses on photoinduced energy transfer in self-assembled multichromophoric supramolecular systems.*



**Christoph A. Schalley**

*Christoph Schalley studied chemistry at the University of Freiburg/Germany and graduated in 1993 from TU Berlin. In his PhD work with Helmut Schwarz, he received his education as a mass spectrometrist and gas-phase chemist. After postdoctoral work on supramolecular chemistry with Julius Rebek at The Scripps Research Institute, La Jolla, USA, he combined both topics when starting his own research group at the University of Bonn. In 2005, he was appointed professor of organic chemistry at FU Berlin. The Schalley group's research topics are diverse and comprise supramolecular chemistry in the gas phase as well as in solution and at interfaces.*
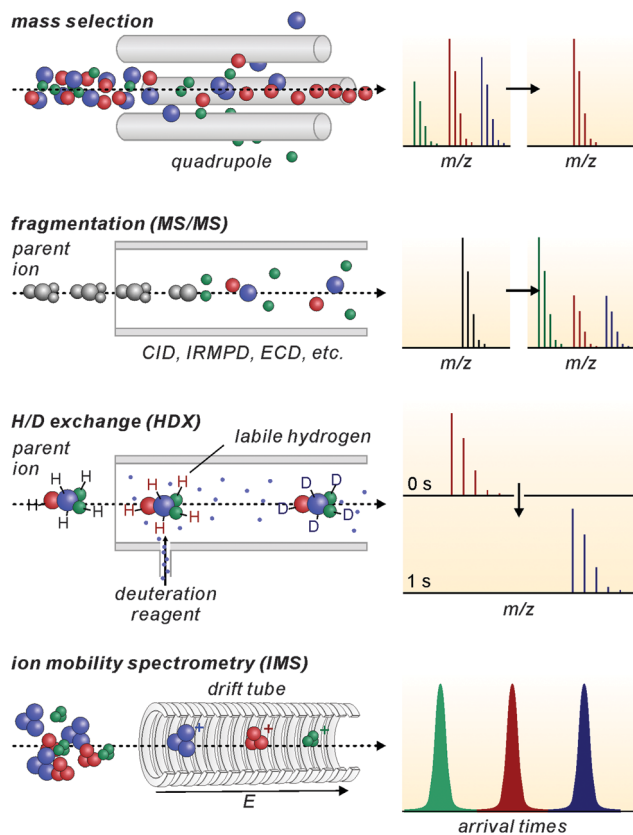
**516** | *Chem. Soc. Rev.,* 2015, **44**, 515–531

This journal is © The Royal Society of Chemistry 2015

**Fig. 2** Schematic illustration of some common tandem MS (MS/MS) experiments. After the mass-selection step (top), fragmentation reactions (second row) or bimolecular reactions (third row) can be performed with the isolated parent ions. A separation by the ions' collision cross sections is possible with ion mobility spectrometry mass spectrometry (bottom), in which the ions are pulled through a gas-filled drift tube with low electric fields.

an example. Undesired ions (blue and green) formed in the ion source travel on unstable trajectories and do not reach the end of the quadrupole, while the parent ion of interest (red) can further be manipulated after this selection step. Once the desired ions are isolated, different fragmentation experiments (Fig. 2, second row) can be performed, among them collision-induced dissociation (CID), infrared multiphoton dissociation (IRMPD), electron-capture dissociation (ECD) or blackbody infrared dissociation (BIRD). Carefully interpreted fragmentation data contain information on many aspects of the ions under study. For supramolecular complexes, the stoichiometry and arrangement of the non-covalently bound subunits in the complex relative to each other can be acquired. Thermodynamic aspects, *e.g.* the stability of the complex ions or a ranking of binding energies in the gas phase, can also be elucidated. Furthermore, mechanistic information on the fragmentation pathways can be obtained. Isotopic labelling is often very helpful for the interpretation of the fragmentation data. However, not only fragmentation reactions are possible. In ion trap or Fourier-transform ion-cyclotron-resonance (FTICR) mass spectrometers, also bimolecular reactions with sufficiently volatile neutral reactants can be performed. H/D-exchange reactions are a prominent example (Fig. 2, third row).[25] Recently, H/D-exchange experiments even revealed how

dynamic supramolecular complexes can be and how mobile their subunits are.[26] Finally, ion mobility spectrometry mass spectrometry (IMS-MS; Fig. 2, bottom) is a quickly growing technology, since commercial instruments have become available. Briefly, ions of interest are pulled by a low electric field or a so-called traveling wave through a gas-filled drift tube. The larger the collision cross section of the ion, the later it arrives at the detector. Consequently, the arrival time distributions contain size information. Although these experiments have not seen extensive use in the characterisation of molecular containers, they are capable of separating isomeric ions of the same $m/z$, if they differ sufficiently in collision cross section.

After this more general introduction into the gas-phase chemistry of supramolecular complexes and the methodology used for its examination, this review will focus on the characterisation and investigation of molecular containers, their structure and reactivity by mass spectrometry. The examples are taken mostly, but not exclusively, from the areas of hydrogen-bonded and metallo-supramolecular containers.

## 2 Analytical and structural characterisation of supramolecular containers

In this section, we focus on metallo-supramolecular and hydrogen-bonded containers. They certainly form the two most prominent groups as both types of interaction, metal coordination and hydrogen bonding, are directional and thus provide geometric control in self-assembly reactions.

**Metallo-supramolecular cages**

An efficient ionisation of containers and their host–guest complexes is the prerequisite for any mass spectrometric experiments to be done with them. Electrospray ionisation (ESI) is certainly the standard ionisation method. For weakly bound metallo-supramolecular complexes, coldspray ionisation (CSI) is very useful.[27] This variant of ESI, in which the sample solution and the ion source are cooled, generates ions with lower internal energies that are less prone to fragmentation. Intact cages can thus be produced, which are otherwise already fragmenting to a large degree under common ESI conditions. Another ESI variant is sonic spray ionisation (SCI-MS) which was also used successfully to ionise fragile metallo-supramolecular cages.[28] Many metallo-supramolecular assemblies contain transition metal cations and are easily ionised by stripping off counterions. When the ligand itself is the counterion and cannot easily be stripped off – like in Beer's resorcinarene-based polymetallic nanocages[29] – an oxidation of one or more metal ions in the sample prior to ionisation can offer an alternative.

Often, signals are observed that can be attributed to fragments of the cages. However, there is a second potential reason for their appearance. ESI concentrations are usually in the low μM regime. When metallo-supramolecular complexes start to dissociate at such low concentrations, incomplete assemblies may be observed just because they already exist in the sample

solution at this low concentration, not because they are due to fragmentation. Increasing concentration to, *e.g.* 100 to 300 μM can be advantageous, even if the ion source then requires more extensive cleaning.

Fujita's lab has extensively utilised coldspray ionisation to examine metallo-supramolecular containers. Fig. 3 (top) shows a series of $M_nL_{2n}$ cages[10,30,31] which were prepared from bent ligands bearing two pyridyl groups and square-planar Pd(II) ions. Characteristic NMR signal shifts indicate complexation of ligand and metal ion, but do not as easily deliver size information unless, for example, extensive DOSY NMR experiments are performed. CSI-MS provides this information easily (Fig. 3, bottom). In all

spectra, a charge-state distribution is observed related to different numbers of stripped-off counterions. Well-resolved isotopic patterns are in line with the calculated ones. Not unexpectedly when considering the low ion source temperatures, some of the ions also carry some solvent molecules. Endohedral functionalization of, for example, the $M_{12}L_{24}$ cage with 24 identical groups such as photo-responsive azobenzene[32] or perfluoroalkyl chains[33] increases the molecular mass significantly. CSI-MS still delivers conclusive mass information.

Their ability to selectively encapsulate guests in their void interior space is an intriguing property of molecular containers.[8a,34] Nitschke's self-assembled porphyrin-faced $M_8L_6$ cubic cage revealed interesting selectivity for the encapsulation of large aromatic guests (Fig. 4).[35] Container Ni-**1** with its cavity volume of *ca.* 1340 Å$^3$ can encapsulate a stack of three coronenes or one fullerene molecule. Mass spectrometry provides clear evidence for target complex formation in agreement with NMR spectroscopy. Cage Ni-**1** has a binding preference for $C_{70}$ and a coronene triple over $C_{60}$. The addition of coronene (3.5 equiv.) or $C_{70}$ (2 equiv.) to a DMF solution of $C_{60}$-saturated Ni-**1** leads to the complete replacement of $C_{60}$ as determined by ESI-MS as well as $^1$H NMR spectroscopy. After the addition of fullerene soot, neither empty cages nor $C_{60}$-filled containers, but rather cages loaded with $C_{70}$, $C_{76}$, $C_{78}$, $C_{82}$ and $C_{84}$ were observed by ESI-MS.

When structural assignments are to be supported by mass spectrometric experiments, specific complexation needs to be distinguished from so-called unspecific binding which frequently occurs in ESI mass spectrometry. Often, changes in sample concentration already provide insight into this matter, but tandem mass spectrometry can also contribute significantly as exemplified by the metallo-supramolecular [7]catenane $M_4A_6B_6$ in Fig. 5.[36] Each edge of the tetrahedron bears one naphthalene diamide (NDI) ligand which can thread through bis-1,5-(dinaphtho)-[38]crown-10 **B**. Consequently, one expects the $M_4A_6B_6$ tetrahedron to be the largest complex in the series. Nevertheless, complexes up to $M_4A_6B_{11}{}^{8+}$ are observed in the ESI mass spectra and one structure-related question is certainly how many crown ethers are threaded and thus bound by mechanical bonds. Infrared multiphoton-dissociation (IRMPD) experiments provide an answer: while $M_4A_6B_6{}^{8+}$ fragments through two competing pathways, *i.e.* the loss of a crown-ether and the charge-separation-driven dissociation of the tetrahedral scaffold into two $M_2A_3B_3{}^{4+}$, $M_4A_6B_7{}^{8+}$ exclusively loses a crown ether first and then continues to fragment just like the $M_4A_6B_6{}^{8+}$ ion. The loss of the first crown ether from the $M_4A_6B_7{}^{8+}$ ion is thus energetically more favourable than the crown ether loss from $M_4A_6B_6{}^{8+}$. The conclusion is that $M_4A_6B_6{}^{8+}$ bears six threaded crowns which require the tetrahedron to open prior to dissociation, while the seventh crown ether is not threaded and thus easily lost without opening the complex.



**sphere 1**
$M_6L_{12}$

**sphere 2**
$M_{12}L_{24}$

**sphere 3**
$M_{24}L_{48}$

**sphere 1**

[M-(CF$_3$SO$_3$)$_7$+DMSO]$^{7+}$

[M-(CF$_3$SO$_3$)$_6$]$^{6+}$

[M-(CF$_3$SO$_3$)$_5$]$^{5+}$

1.0 amu

[M-(CF$_3$SO$_3$)$_6$+(DMSO)$_2$]$^{8+}$

[M-(CF$_3$SO$_3$)$_6$]$^{6+}$

1224 1225 1226 1227 1228

800 1000 1200 1400 1600 m/z

**sphere 2**

10+

11+

12+

13+

9+

8+

7+

6+

700 900 1100 1300 1500
*m/z*

**sphere 3**

18$^+$ 17$^+$

19$^+$

20$^+$

21$^+$

22$^+$

23$^+$ 24$^+$ 25$^+$ 26$^+$ 27$^+$ 28$^+$

16$^+$

15$^+$

700 900 1100 1300 m/z

**Fig. 3** CSI mass spectra of Fujita's $M_nL_{2n}$ **sphere 1** ($n$ = 6), **sphere 2** ($n$ = 12), and **sphere 3** ($n$ = 24) metallo-supramolecular capsules. Adapted and reproduced from ref. 10, 30 and 31 with kind permission by the American Association for the Advancement of Science, the Royal Society of Chemistry and Wiley-VCH.

## Hydrogen-bonded capsules

Because of its usually somewhat harsher ionisation conditions, matrix-assisted laser desorption/ionisation (MALDI) has very rarely been used with success to ionise hydrogen-bonded
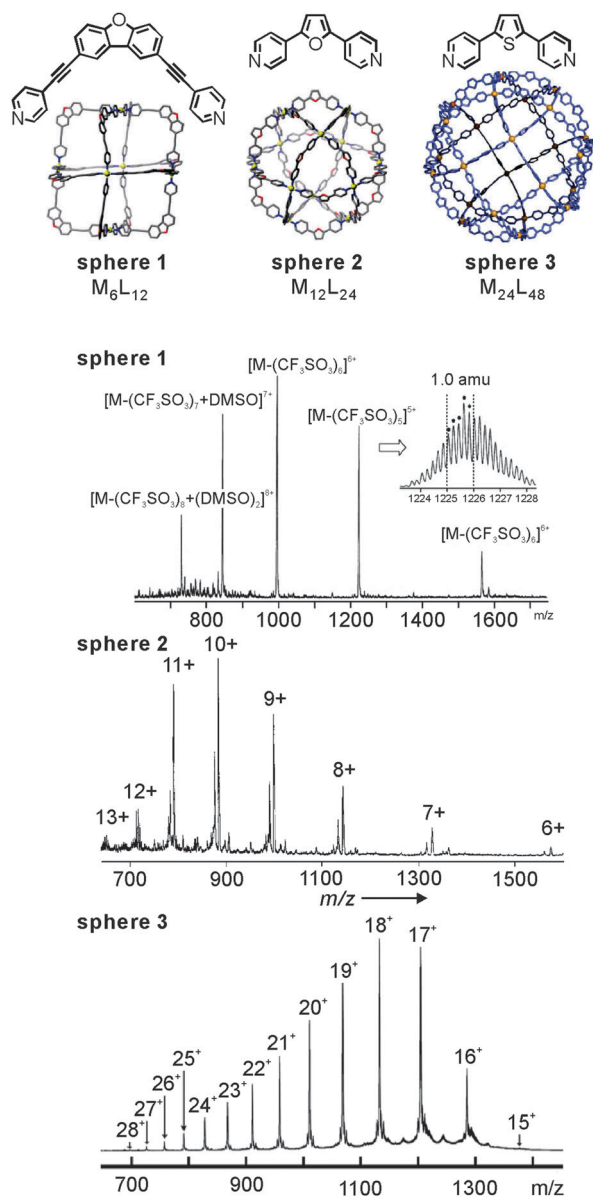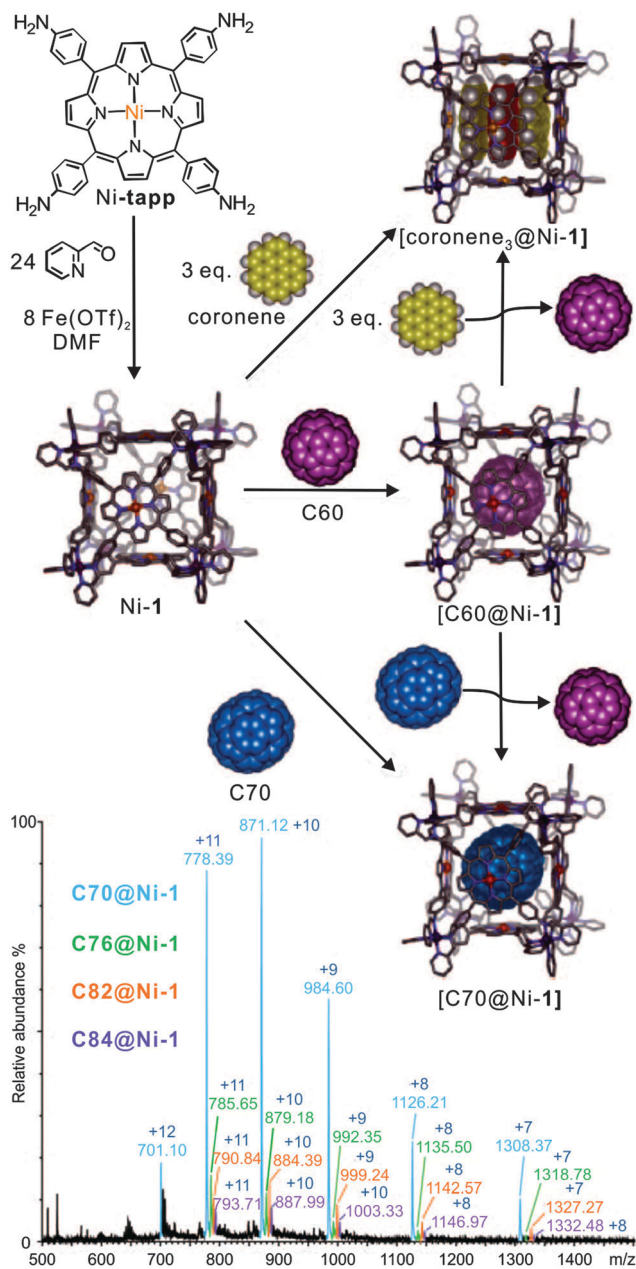
518 | *Chem. Soc. Rev.*, 2015, **44**, 515–531

This journal is © The Royal Society of Chemistry 2015

Fig. 4 The synthesis of cubic cages Ni-**1** through subcomponent self-assembly. The resulting cage hierarchically forms host–guest inclusion with coronene, $C_{60}$, and $C_{70}$. $C_{70}$ and coronene guests bind more strongly than $C_{60}$. The bottom ESI-MS shows the result of mixing fullerene soot with Ni-**1**. Adapted and reproduced from ref. 35 with kind permission by Wiley-VCH.



Fig. 5 (a) Synthesis of $M_4A_6$; (b) representation of a dynamic combinatorial library (DCL) formed upon addition of excess crown ether **B**. (c) ESI-FTICR mass spectrum of $M_4A_6$. Insets show isotope patterns of $m/z$ 612 after mass-selection at different time intervals of irradiation in an IR multiphoton dissociation experiment. The gradual growth of the $[M_2A_3]^{4+}$ ion (peak spacing of 1/4 amu) at the expense of the $[M_4A_6]^{8+}$ parent ion, indicating the imposed $[M_2A_3]^{4+}$ ions are the fragmentation product during the ionisation process. The similar fragmentation also occurred for the $[M_4A_6B_6]^{8+}$ parent ion. (d) ESI-FTICR mass spectrum of a 1:10 cage–crown ether mixture. (e,f) Spectra obtained from IRMPD experiments performed with mass-selected $[M_4A_6C_6]^{8+}$ and $[M_4A_6C_7]^{8+}$ ions, respectively. Adapted and reproduced from ref. 36 with kind permission by Wiley-VCH.

containers. One notable example is certainly the barbiturate/melamine stacks made by Reinhoudt *et al.*[37] When hydrogen-bonded containers are to be investigated by the softer ESI-MS, one nevertheless frequently encounters the difficulty that non-competitive, rather unpolar solvents are not the best spray solvents for electrospray ionisation. *Vice versa*, polar organic solvents that are good spray solvents often lead to the dissociation of the desired complexes. In addition, charge labelling is required, if the capsule is neutral. The encapsulation of charged
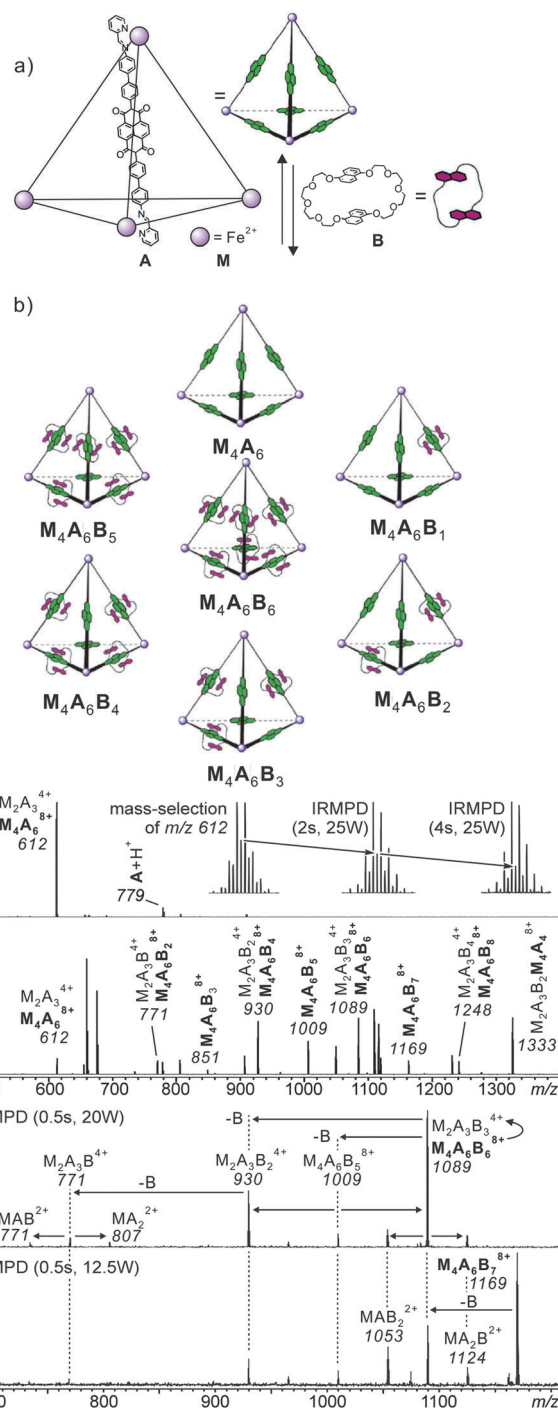
guests is a convenient way to approach both problems.[38] On the one hand, the necessary charge is present inside the cavity of the capsule and stripping off the non-encapsulated counterion is quite easily possible. On the other hand, the non-covalent interactions between the ion inside the container and the container walls are usually stronger than those of an equivalent neutral guest and thus stabilise the container. This usually allows adding at least a few percent of a polar solvent to the sample thus facilitating the electrospray process.

Rebek's softballs (Fig. 6) illustrate this.[1a] Monomers **S1–S4** consist of two glycoluril binding sites connected by spacers of different lengths. The corresponding dimers thus bear differently sized cavities. ^{1}H NMR studies in aprotic, unpolar solvents like chloroform or xylene provided evidence for dimer formation as well as the encapsulation of suitable guests. In order to detect the dimeric capsules by ESI-MS, quaternary ammonium ions with weakly coordinating counterions ($BF_4^-$, $PF_6^-$) were used for ion labelling.[39] With the same strategy, other hydrogen-bonded capsules – the tetrameric "footballs",[40] the so-called flexiballs,[41] in which the binding sites are connected

to a central scaffold in a less rigid fashion by single bonds, cavitand-based capsules large enough to encapsulate host–guest complexes thus forming Matroshka-doll-like molecule-in-molecule-in-molecule complexes[42] and tetraurea calixarene capsules[43] – were successfully ionised.

Evidence for intact capsular structures with guests residing inside the capsules' cavities came from a series of experiments that demonstrated (i) guest binding to be size-selective, (ii) capsule formation not to occur for deformed capsule monomers or monomers with protected binding sites and (iii) covalent bond cleavage to be energetically competitive in the gas phase with the loss of the guest cation. The latter fragmentation experiment indicates the barrier of guest loss to be high – well consistent with a steric barrier created by the capsule walls that need to be opened prior to guest release.

Resorcinarene **Re** and pyrogallarene **Py** shown in Fig. 7 also form dimeric capsules,[44] when a sufficiently small guest cation such as tetramethyl ammonium is encapsulated. With larger guests such as tetrahexyl ammonium or cobaltocenium, hexameric capsules are instead observed in solution and solid state. They bear one resorcinarene or pyrogallarene on each of the six faces of a cube.[11,12,45] The resorcinarene hexamers carries eight water molecules on the corners of the cube completing the hydrogen bonding pattern. The cavity volume reaches 1200 $Å^3$. Similar in size, the pyrogallarene hexamers does not require any water molecules to complete H-bonding.

Mass spectrometric studies of pyrogallarenes and resorcinarenes clearly reveal the choice of the templating guest cation to be decisive for hexamers formation.[46] Electrospray ionisation of **Py** alone shows a series of unspecific oligomers to form (Fig. 7a). When small cations such as tetramethyl ammonium are added, dimers are the exclusive product (Fig. 7b). Larger cations with unfavourable symmetry like tetrabutyl ammonium lead to the formation of a series of larger oligomers. They include hexameric complexes, but their formation is not specific (Fig. 7c). When a pseudo-octahedral guest such as $Ru(bpy)_3^{2+}$ is used which fits the cavity size and the symmetry of the hexameric capsule, the hexamer is almost the only product formed (Fig. 7d). Apparently, the formation of a hexameric capsule requires an appropriate template that fits into the cavity of this capsule with respect to size and symmetry. Control experiments with tetramethylated resorcinarene did not yield any hexamers. Evidence for the capsular structure and the guest dication located inside the capsule came from IRMPD experiments performed with mass-selected hexamers. They show guest release only to occur after the loss of three monomers. This is clearly in contrast to the structure of an empty capsule with the guest cation bound to the outer surface. For such an isomer, one would expect facile loss of the complete hexamers.
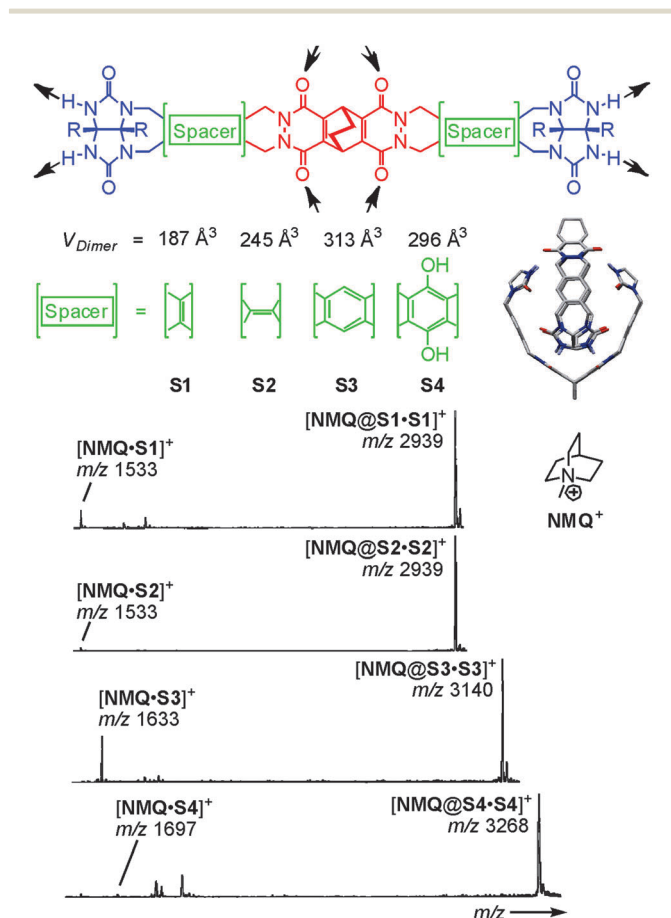


**Fig. 6** Top: chemical structures of the self-complementary building blocks present in molecular softballs. Arrows: H bond donors and acceptors. Right: force-field-optimized structure of the H-bonded dimeric capsule **S3·S3**; solubilizing R groups (*n*-heptylphenyl) and carbon-bound H atoms are omitted for clarity. Bottom: ESI mass spectra of 50 mM chloroform solutions of softballs **S1·S1–S4·S4** with 1 eq. of guest cation **NMQ**[+]. Adapted and reproduced from ref. 39 with kind permission by Wiley-VCH.

# 3 Monitoring solution reactivity by electrospray ionisation mass spectrometry

After discussing the intact ionisation and providing a few selected examples on the question how the structure of supramolecular
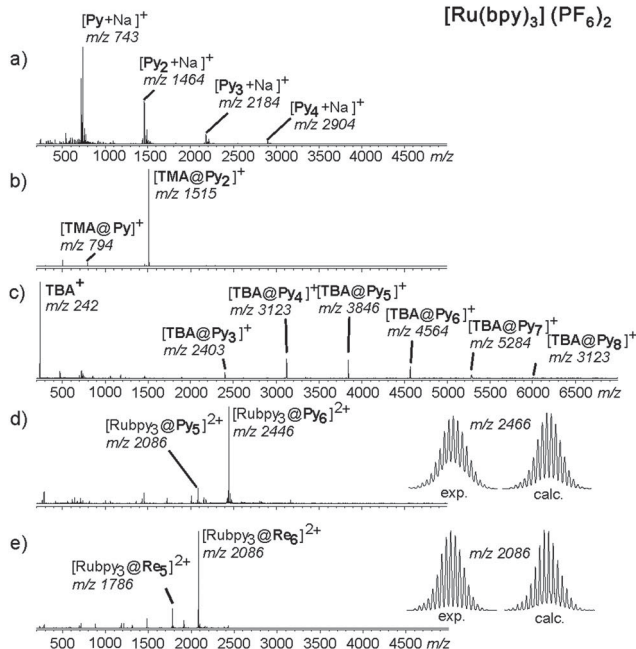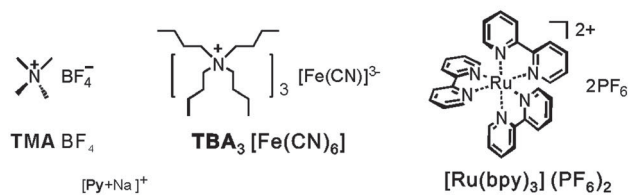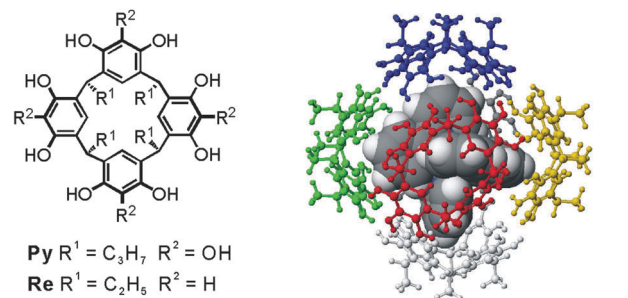
**Fig. 7** Encapsulation of ionic guests by a pyrogallarene capsule is used in order to investigate the complex by ESI-FTICR. ESI-FTICR mass spectra of (a) **Py**, (b) after addition of **TMA**BF$_4$, (c) **TBA** [Fe(CN)$_6$]$^{3-}$ and (d) Ru(bpy)$_3$(PF$_6^-$)$_2$. (e) Same ESI-FTICR mass spectrum recorded with **Re** instead of **Py**. Insets: experimental and calculated isotope patterns of the hexamer ions [Ru(bpy)$_3$@**Py**$_6$]$^{2+}$ and [Ru(bpy)$_3$@**Re**$_6$]$^{2+}$. Adapted and reproduced from ref. 46 with kind permission by Wiley-VCH.

containers can be approached by mass spectrometric experiments, we will now address mass spectrometric experiments which monitor reactions of containers in solution. We choose two processes as examples: building block exchanges in metallo-supramolecular containers and self-sorting phenomena in hydrogen-bonded dimeric tetraurea calixarene capsules.

### Building block exchange processes

Ligand exchange reactions are a characteristic dynamic feature of most metallo-supramolecular assemblies.[47] The first case to be discussed here is that of self-assembled metallo-supramolecular squares decorated with **G0** to **G3** Frèchet dendrons (Fig. 8).[48] The hydrophobic dendrons surround a nanometre-sized cavity at the
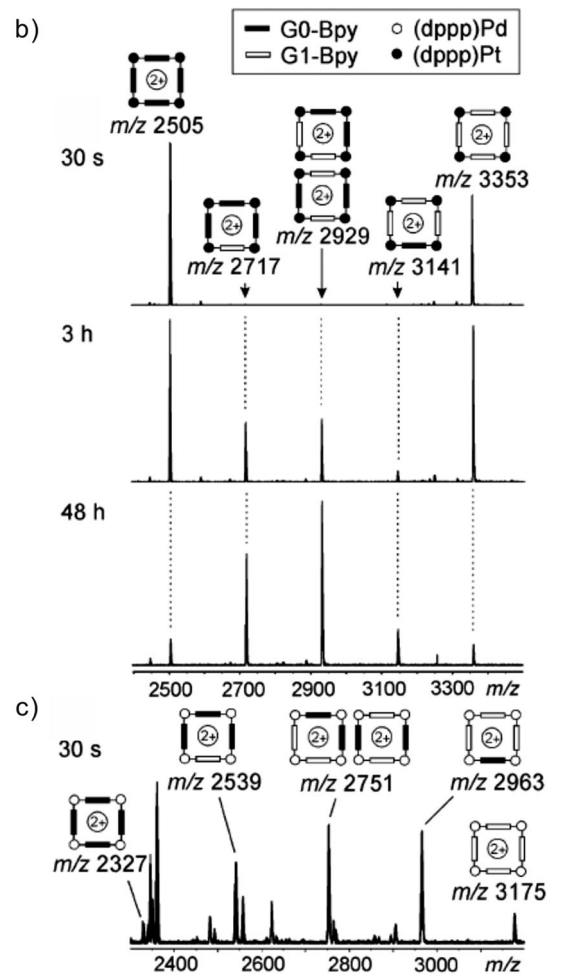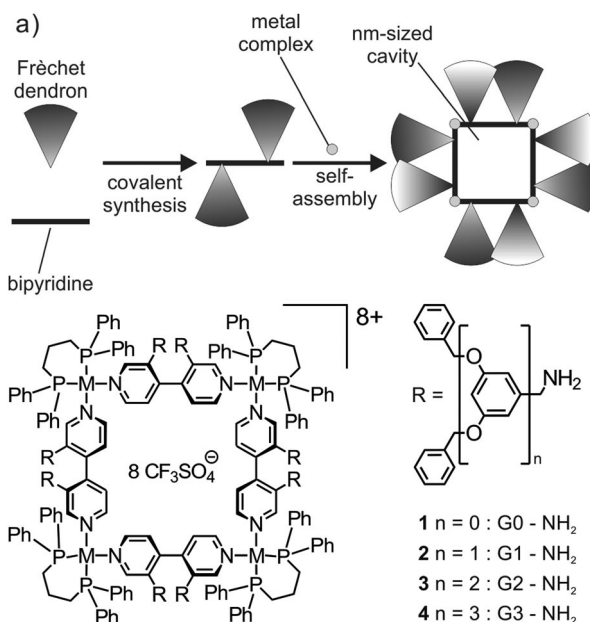


**Fig. 8** (a) Self-assembled metallo-supramolecular dendrimers: 4,4′-bipyridines bearing Frèchet dendrons assemble with the appropriate metal corners to yield dendron-decorated squares with a nanometre-sized hydrophobic cavity. ESI-FTICR mass spectra of 1:1 mixtures of (b) **G0** and **G1** Pt(II) squares 30 s, 3 h and 2 days after mixing and (c) **G0** and **G1** Pd(II) squares 30 s after mixing both squares. Adapted and reproduced from ref. 48 with kind permission from Wiley-VCH.

This journal is © The Royal Society of Chemistry 2015

Chem. Soc. Rev., 2015, **44**, 515–531 | 521

core of the assemblies and eight amide-groups inside this pocket provide hydrogen-bonding sites for guest recognition. The square can form a dynamic library of up to 54 different isomeric squares which differ by the arrangement of the dendrons above and below the square plane. In addition, they can point inwards or outwards due to the torsional angle along the aryl–aryl bond. The corresponding NMR spectra are thus very complicated. However, as all possible isomers for each square have the same elemental composition and thus the same mass, ESI mass spectrometry provides a straightforward characterization.

When two squares with different bipyridine ligands are mixed (*e.g.* mixing independently formed **G0** and **G1** (dppp)Pt(II) squares, Fig. 8b), mass spectrometry can also be used to record the dynamic component exchange process. After the initial mixing and ionisation (*ca.* 30 s), two prominent peaks corresponding to the pre-generated **G0** and **G1** (dppp)Pt(II) squares are observed. Since the exchange process at the Pt centre is rather slow, equilibrium is reached only after *ca.* 2 days and no further intensity changes are observed. Owing to the absence of any cooperative interactions between the dendron moieties, all possible forms ($G0_4 : G0_3G1_1 : G0_2G1_2 : G0_1G1_3 : G1_4$) are observed in the mass spectra in an almost statistical $1 : 4 : 6 : 4 : 1$. Small deviations from this ratio may be associated with different ESI response factors that are due to differences in desolvation energies. In contrast to the Pt(II) complexes, the corresponding (dppp)Pd(II) squares exhibit a rather fast exchange. A complete equilibration is already obtained after less than 30 s (Fig. 8c).

With a similar protocol, Stang *et al.* monitored dynamic ligand exchanges between coordination-driven self-assembled supramolecular polygons by ESI-MS even quantitatively using isotope labelling rather than different substituents to distinguish the two initial assemblies.[49]

Fujita's group employed mass spectrometry to monitor the ligand exchange between large $M_{12}L_{24}$ spherical complexes.[50] This spherical cage is again based on Pd(II)–pyridine interactions. However, this assembly-mode leads to a significantly different kinetic behaviour: as shown in Fig. 9, two spheres, $M_{12}L^A_{24}$ and $M_{12}L^B_{24}$, bear nearly identical ligands which only differ with respect to the endohedral alkyl chains ($n$-$C_3H_7$ and $n$-$C_6H_{13}$ for $L^A$ and $L^B$, respectively). Immediately after mixing, the two independently generated spheres in a 1:1 ratio, two similarly intense signals are observed corresponding to the two homo-24mers. Apparently, ligand exchange is rather slow. Time-dependent mass spectrometric experiments reveal a quite remarkable kinetic stability of the spheres against ligand exchange. Over longer reaction times, the first ligand exchange is observed with rather low abundance and has a half-life of *ca.* 20 days. In a second experiment, in which a free ligand was added to the previously prepared sphere of the second one, a much faster exchange process operates with a half-life for the first ligand exchange of *ca.* 23 min. The ligand exchange on tetracoordinate mononuclear metal complex $[Pd(py)_4](OTf)$ even occurs with a half-life of 36 s. Consequently, cooperative behaviour due to the fully closed coordination complex slows down the ligand exchange process. These experiments nicely show that ESI mass spectrometry can provide more profound
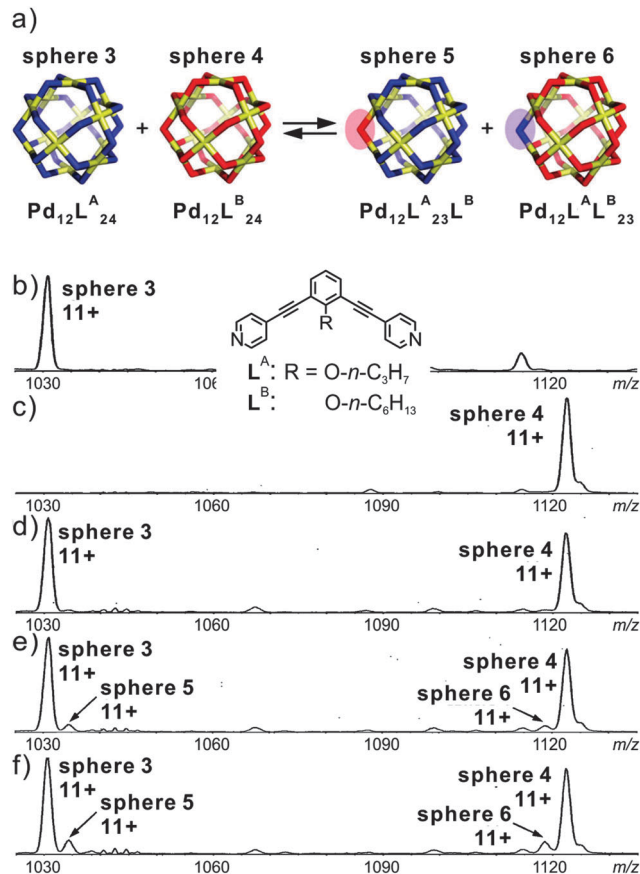


**Fig. 9** (a) Schematic representation of the ligand exchange between **sphere 3** and **sphere 4**. (b) and (c) CSI-MS spectra (CH$_3$CN, triflate salt) showing the expanded regions of the 11+ signal for **sphere 3** and **sphere 4**. Time dependent spectra recorded after keeping the sample (d) overnight, (e) for 35 h, and (f) for 70 h at room temperature. Reproduced from ref. 50 with kind permission by the American Chemical Society.

insight into exchange processes in solution and at least produces semi-quantitative kinetic data.

## Self-sorting of tetraurea calixarene capsules

Recently, Böhmer's and our groups have reported a self-sorting system based on dimeric hydrogen-bonded tetraurea calixarene capsules made from **U1–U11**.[51] As shown in Fig. 10, the dimerisation of eleven tetra-urea calix[4]arenes is controlled by steric factors. Many dimers are unable to form when both monomers bear wrongly positioned loops that would need to catenate upon dimerization. As catenation is not possible without breaking at least one covalent bond, these dimers do not form. Analogously, other monomers carry bulky stopper groups unable to penetrate the loops. Again, a mismatch of looped with stoppered monomers rules out the formation of a number of dimers. Following these simple rules, 35 possible dimers can be formed (Fig. 10b). When stoichiometry is controlled in addition to these steric effects, the number of dimers can further be reduced to six, because **U11** can only bind to **U1** and thus fully consumes this monomer. Among the remaining
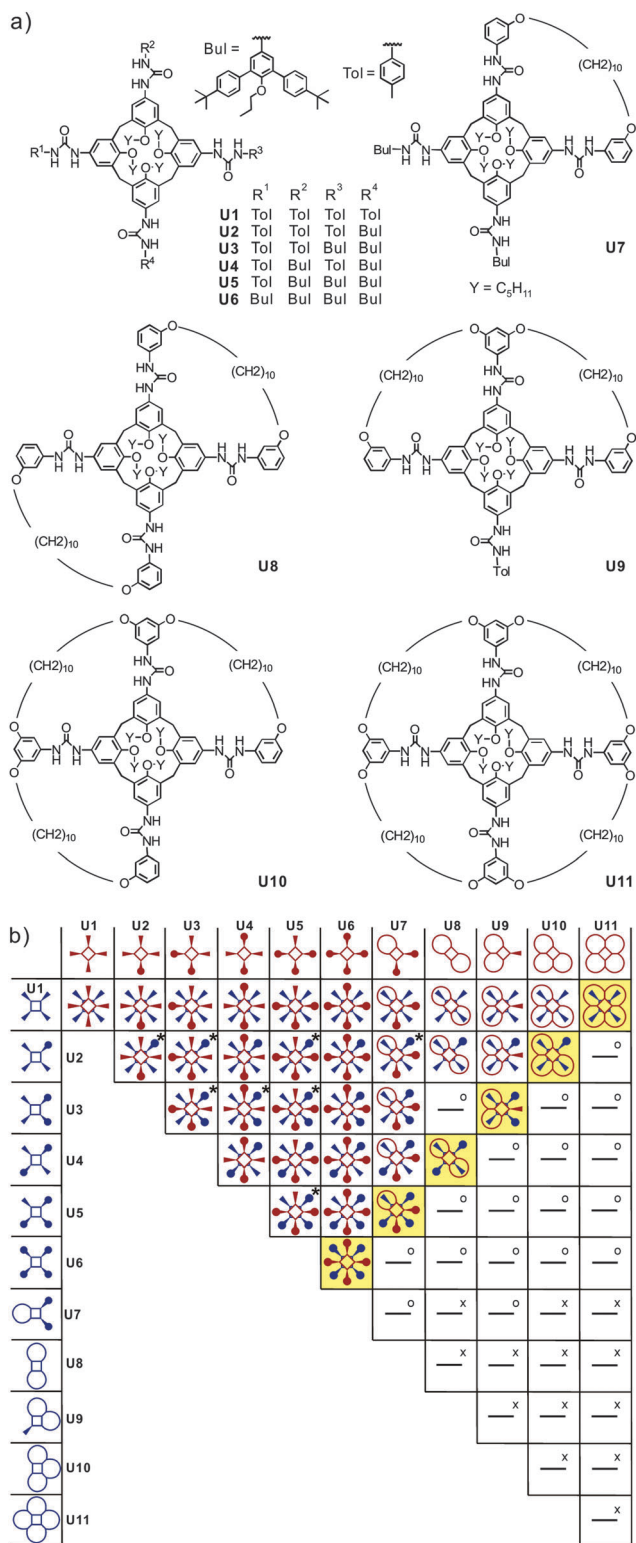
**Fig. 10** (a) Eleven tetraurea calix[4]arenes **U1–U11** and (b) table containing the expected outcome of the self-sorting processes occurring in a stoichiometric mixture of all monomers **U1–U11**. Dimeric combinations marked "x" are impossible because of overlapping loops, while "o" indicates the impossibility of bulky residues to penetrate these loops. Two or three regioisomers are possible for dimers marked "x". Adapted and reproduced from ref. 51 with kind permission by Wiley-VCH.

monomers, **U10** can only bind to **U2** *etc.* Finally, only the six dimers highlighted in yellow in Fig. 10 are expected to emerge.

For simpler mixtures of only a selection of two or three of these tetraurea calixarene monomers, NMR spectroscopy is still able to provide clear evidence for such self-sorting mixtures.
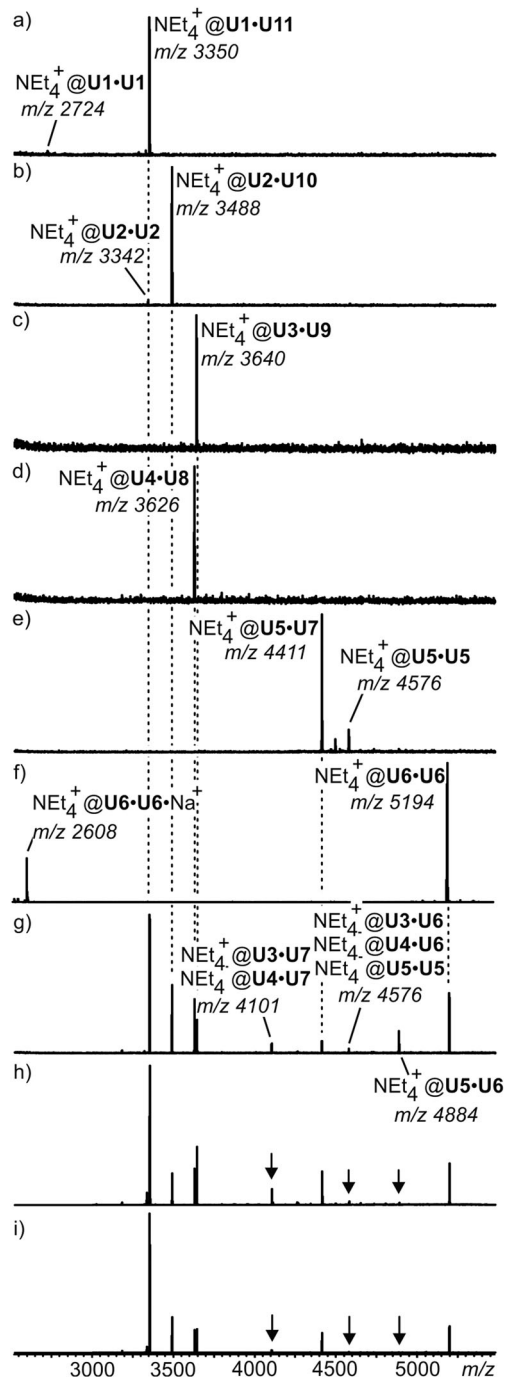


**Fig. 11** ESI mass spectra of equimolar mixtures of (a) **U1·U11**, (b) **U2·U10**, (c) **U3·U9**, (d) **U4·U8**, and (e) **U5·U7**. (f) **U6·U6**. (g) ESI mass spectrum of an equilibrated mixture of all eleven monomers. (h,i) Spectra of the same mixture with 10% and 20% excess of loop-containing monomers **U7–U11**, respectively. For ion labelling, each capsule contains one tetraethyl ammonium ion as the guest. Reproduced from ref. 51 with kind permission by Wiley-VCH.

This journal is © The Royal Society of Chemistry 2015

Chem. Soc. Rev., 2015, 44, 515–531 | 523

However, when all monomers are mixed, an analysis by NMR becomes difficult. Using ion labelling with tetraethyl ammonium, mass spectrometry can then be used for the investigation of this mixture. Indeed, self-sorting in solution clearly occurs (Fig. 11). One result is that it takes several days to reach the final equilibrium. However, some minor signals with intensities lower than *ca.* 5% appear that can be assigned to mismatched dimers, which are not expected to form in a perfect self-sorting system. These signals may be due to a minor amount of unspecific dimerization. When a slight excess of the looped monomers is added, the mismatched dimers vanish and only the signals for the expected capsules are observed. This example illustrates how mass spectrometry helps to analyse self-sorting in rather complex mixtures. It thus adds valuable insight complementary to that obtained with other methods.

# 4  Gas-phase experiments aiming at the investigation of intrinsic ion reactivity

In comparison to solution, the high vacuum inside the mass spectrometer provides a very different environment. The absence of solvation strengthens most non-covalent interactions as there is no competition with the solvent molecules. Experiments performed after mass-selecting an ion of interest therefore provide valuable insight into the intrinsic properties of the containers under study. Also, the dynamic subunit exchange processes discussed above are efficiently suppressed in the gas phase and intramolecular reactivity is observed rather than intermolecular exchange processes.[52] This part commences with fundamental binding studies on resorcinarene containers followed by a mechanistic analysis of cage contraction processes that occur in the gas phase. Finally, bimolecular reactions, *i.e.* the gas-phase H/D-exchange will provide mechanistic as well as structural features on resorcinarene host–guest complexes and hydrogen-bonding in resorcinarene and pyrogallarene capsules.

### Fundamental binding studies: the importance of C–H···anion interactions

A number of different methods for the evaluation of gas-phase binding data exist, many of which, however, have not yet been applied to capsules and containers. Schrader and co-workers have examined a series of electrostatically bound calixarene-based capsules with respect to their relative stabilities[53] and used collision experiments during which the collision energy was gradually increased. Determining the point at which 50% of the capsules are destroyed ($CE_{50}$ value) provides a measure for its stability. The ranking of the stability of different capsules gained in the gas-phase correlates quite nicely with that determined from NMR titrations revealing the solvation effects to be of minor importance compared to the non-covalent interactions between the two electrostatically bound monomers.

A similar strategy was utilized to unravel the importance of C–H···anion interactions[54] in resorcinarene cavitands. While resorcinarenes themselves are cation binders, the corresponding

cavitands (Fig. 12) turned out to bind anions rather than cations.[55] Even weakly bound anions such as $PF_6^-$ form complexes upon electrospray ionisation with a calculated binding energy of *ca.* 25 kJ mol$^{-1}$. Even the complexation of sulphate dianions,
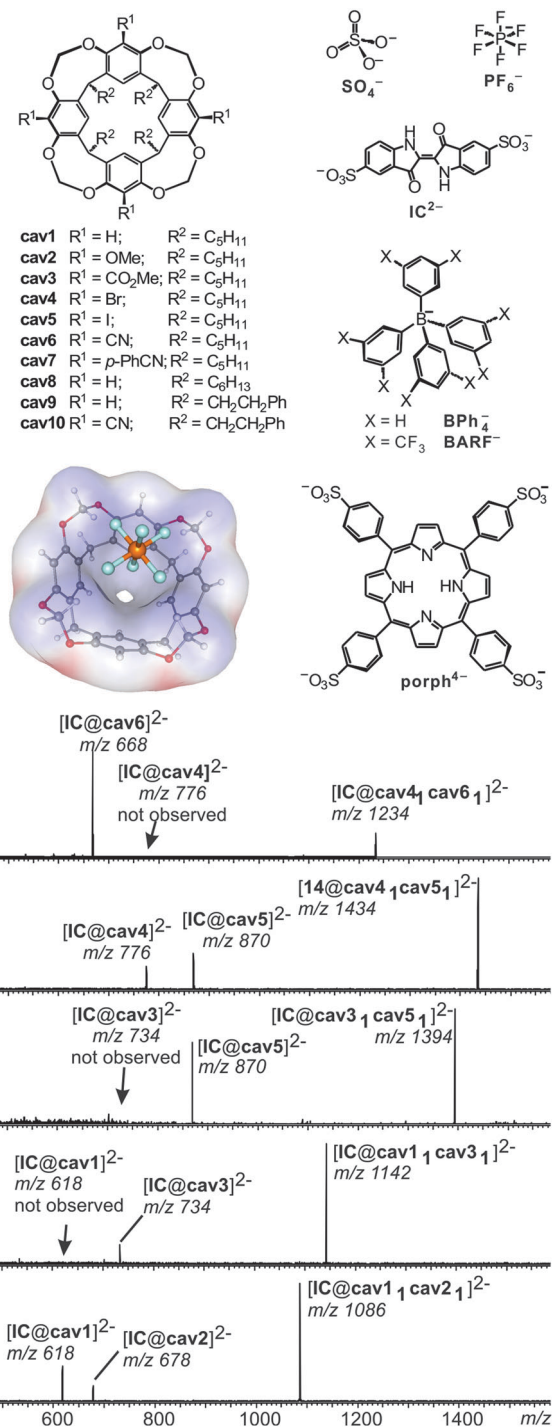


**Fig. 12**  Top, left: anion-binding cavitands **cav1–cav10** and B3LYP/6-31++G(d,p)-optimized structure of complex [$PF_6$@**cav1**]$^-$ with the electrostatic potential mapped on the host's van der Waals surface. Top, right: guest anions. Bottom: CID experiments with mass-selected, doubly charged heterodimeric **IC**$^{2-}$ complexes. Adapted and reproduced from ref. 55 with kind permission by Wiley-VCH.

which do not exist unsolvated in the gas phase due to an instantaneous electron loss, is observed in complexes such as $[SO_4@cav1]^{2-}$ and $[SO_4@cav1_2]^{2-}$. Obviously, solvation of the sulphate dianion by the cavitand is sufficiently strong to stabilize it efficiently. Likely, multiple C–H···anion interactions between the methylene groups at the rim and the anion lead to quite significant binding energies that – according to calculations – need to be in the range of $\sim$130 to 160 kJ mol$^{-1}$ for an efficient stabilization of the sulphate dianion.

In order to investigate substituent effects at the cavitand's aromatic rings, indigo carmine $IC^{2-}$ has been used as the guest. This dianion forms homo- and heterodimers when mixed with two differently substituted cavitands. Mass-selection of the heterodimer followed by collision-induced fragmentation allows comparing the two different cavitands incorporated in the complex directly. The less strongly bound cavitand dissociates to a greater extent and thus the relative peak intensities of the two possible 1:1 cavitand/$IC^{2-}$ product ions provide a direct measure of the relative gas-phase binding energy ranking. In agreement with the expected substituent effects, anion binding strengths increase in the series OMe $\leq$ H $\ll$ CO$_2$Me $\ll$ Br $\approx$ I $\ll$ CN, i.e. from electron-donating to electron withdrawing substituents. Mass spectrometry consequently provides a means to conduct fundamental binding studies even on complexes that do not exist in solution due to the competition with solvent molecules or ion pairing effects.

## Mechanistic analysis of intramolecular processes: a double cage contraction in the gas phase

As outlined above, one unique feature of gas-phase studies with mass-selected supramolecular complex ions in the gas phase is the fact that the dynamic equilibria which govern solution reactivity are efficiently suppressed. Consequently, the intramolecular reactivity of the ions of interest can be examined and offers completely new insight that is difficult to obtain from solution studies – if possible at all.

In an earlier study,[56] we were able to demonstrate simple metallo-supramolecular squares to fragment into triangles by a backside attack mechanism as shown in Fig. 13. The analysis was based on IRMPD experiments performed with the triply charged square. For fragmentation, the square needs to be opened first giving rise to a linear tetramer. This tetramer could in principle fragment with similar energy demand at several metal–nitrogen bonds along the chain. Nevertheless, the fragmentation is highly selective for the formation of doubly charged $M_3L_3^{2+}$ triangles and the corresponding singly charged 1:1 $ML^+$ complex. Other fragmentation channels, e.g. the formation of two $M_2L_2$ fragments were not observed. The energetic preference for only one of the possible fragmentation reactions can be rationalized by a "backside-attack" mechanism: within the linear tetramer, the free pyridine coordination site first forms a new M–N bond followed by subsequent loss of the $ML^+$ fragment. The binding energy gained by bond formation is thus available in the complex and supports dissociation. Such addition–elimination mechanisms are well-known for ligand exchanges at d$^8$ metal ion complexes. Other pathways
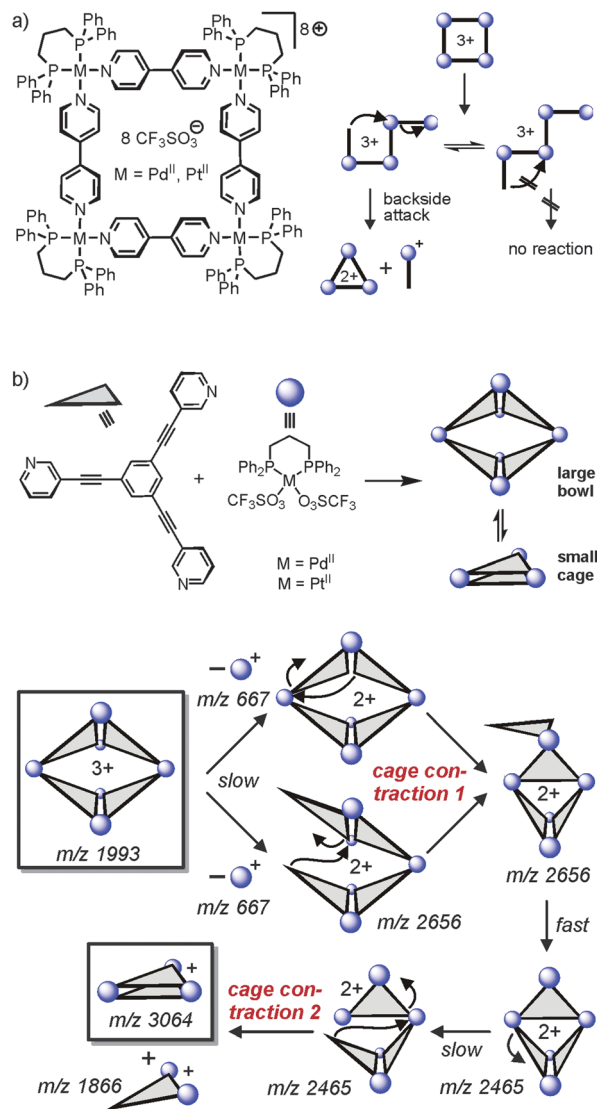


Fig. 13 (a) Fragmentation pathway of metallo-supramolecular squares in the gas phase. A "backside-attack" mechanism rationalizes the strong preference for only one dissociation reaction, although several energetically equivalent fragmentation sites exist within the linear $M_4L_4^{3+}$ complex after ring opening. (b) The same mechanism operates in a double cage contraction process. Adapted and reproduced from ref. 57 with kind permission by the Royal Society of Chemistry.

within the linear tetramer cannot follow such a backside-attack mechanism due to steric reasons and thus fragmentations at other M–N bonds do not benefit from a preceding bond formation and are thus energetically more demanding. Two conclusions can be drawn from these findings: (i) the strain within the triangle structure must be lower than the binding energy of a M–N bond and (ii) the $M_3L_3^{2+}$ product is initially a cyclic triangular structure before it continues to fragment. IRMPD experiments with the bowl-shaped $M_6L_4$ metallo-supramolecular cage shown in Fig. 13b reveal similar fragmentation mechanisms.[57] Two "backside-attack" steps lead to the contraction into smaller cages and finally an $M_3L_2^+$ cage is formed. Most interestingly, it is what is *not*

This journal is © The Royal Society of Chemistry 2015

Chem. Soc. Rev., 2015, 44, 515–531 | 525

observed in the mass spectra which finally leads to this mechanistic analysis.

## H/D exchange reactions: a supramolecular analogue of proton transport in water

H/D-exchange (HDX) experiments in the gas phase can provide detailed information on supramolecular structure and reactivity in particular for hydrogen-bonded complex ions.[25] Mechanistically, a simple HDX reaction occurs in a sequence of five steps: (i) encounter complex formation between the charged substrate and the neutral deuteration agent, (ii) a proton transfer from the substrate to the deuteration agent, (iii) isotope scrambling, (iv) deuteron back-transfer to the substrate and, finally, (v) dissociation of the product complex and loss of the non-deuterated agent. This simple mechanism depends on the proton affinity difference between the substrate and the agent. The larger this difference, the slower the exchange. If a second functional group is present in the substrate, which may actively mediate the process, H/D-exchanges are often much faster, as so-called relay mechanisms[58] become possible.

Vainiotalo *et al.* investigated the H/D-exchange on tetra-sulfonylated resorcinarenes **resoS1** and **resoS2** (Fig. 14) which form 1:1 complexes with the primary, secondary and tertiary ammonium ions **mR**, **dR** and **tR** (R = Me, Et).[59] N–H···O=S hydrogen bonding is certainly important for binding besides cation-π interactions. In these complexes, no exchange is observed for the resorcinarene OH protons when the complexes were reacted with $ND_3$ – likely because they are involved in hydrogen bonding to the sulfonyl groups of the adjacent aromatic rings. Instead, all of the guests' NH protons do exchange. The exchange rates were determined and amount to $k_1 = 2.36 \times 10^{-11}$ cm$^3$ molecule$^{-1}$ s$^{-1}$, $k_2 = 1.71 \times 10^{-11}$ cm$^3$ molecule$^{-1}$ s$^{-1}$ and $k_3 = 7.66 \times 10^{-12}$ cm$^3$ molecule$^{-1}$ s$^{-1}$ for the three exchange steps of $[\mathbf{mEt \cdot resoS1}]^+$ as an example.

Similarly, the phosphonylated cavitands **resoP1–resoP4** (Fig. 14)[60] also bind ammonium ions.[61] These cavitands are much more rigid as compared to **resoS1** and **resoS2** and bear P=O groups converging towards the resorcinarene cavity. HDX experiments help to unravel the binding modes for primary, secondary and tertiary ammonium ions. Using $ND_3$ as the deuteration agent, the exchange reaction is fast for $[\mathbf{mEt@resoP4}]^+$ with a primary ammonium ion as the guest, while it does not occur at all for the corresponding secondary ammonium ion complex $[\mathbf{dEt@resoP4}]^+$. The latter finding is again in contrast to the observation that $[\mathbf{dEt@resoP1}]^+$ and $[\mathbf{dEt@resoP3}]^+$ undergo a fast exchange of both ammonium NH protons.

Clearly, these data are in agreement with the interpretation that the primary ammonium ion binds only to two P=O groups in **resoP4**, while the third N–H proton is available for exchange. A rearrangement within the complex then leads to the formation of one hydrogen and one deuteron bond and thus a second NH proton is available for the exchange. Similarly, the third proton is exchanged in a third step. A secondary ammonium ion instead forms two hydrogen bonds to two P=O groups in **resoP4** and is thus protected against any exchange, because no exchangeable NH proton is left. The same ion can however form only one hydrogen bond to **resoP1** (only one
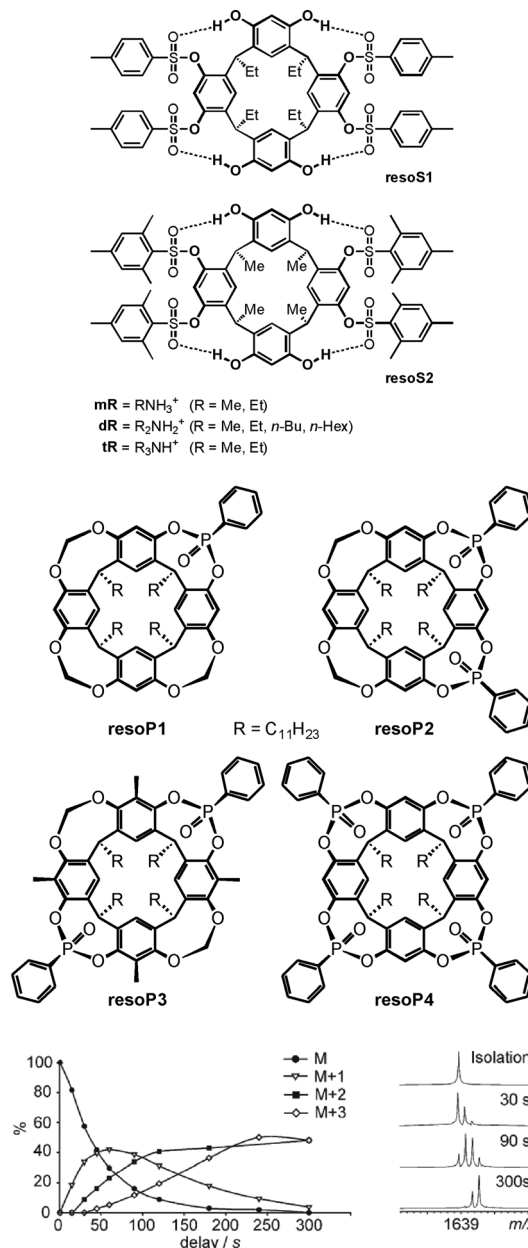


mR = RNH$_3^+$  (R = Me, Et)
dR = R$_2$NH$_2^+$  (R = Me, Et, *n*-Bu, *n*-Hex)
tR = R$_3$NH$^+$  (R = Me, Et)

**resoP1**     R = C$_{11}$H$_{23}$     **resoP2**

**resoP3**                                   **resoP4**

Fig. 14 Tetrasulfonylated (top) and phosphonylated (centre) resorcinarenes whose ammonium ion complexes have been investigated by gas-phase H/D-exchange experiments. Bottom: relative abundances of the parent ion and the H/D-exchange products for the [EtNH$_3$·**resoP4**]$^+$ complex (left) and the corresponding mass spectra after different reaction times (right). ND$_3$ was used as the exchange reagent. Bottom figure adapted and reproduced from ref. 60*a* with kind permission by the Royal Society of Chemistry.

P=O group available) and **resoP3** (unsuitable arrangement of the two P=O groups). These studies nicely show how H/D-exchange experiments unravel details of the binding mode and at the same time provide insight into dynamic processes occurring in container/guest complexes.

When the dimeric resorcinarene capsule $[\mathbf{Cs \cdot reso_2}]^+$ shown in Fig. 15 is subjected to H/D-exchange experiments, one would likely expect based on the complexes discussed above that no significant exchange is observed as all OH groups are involved
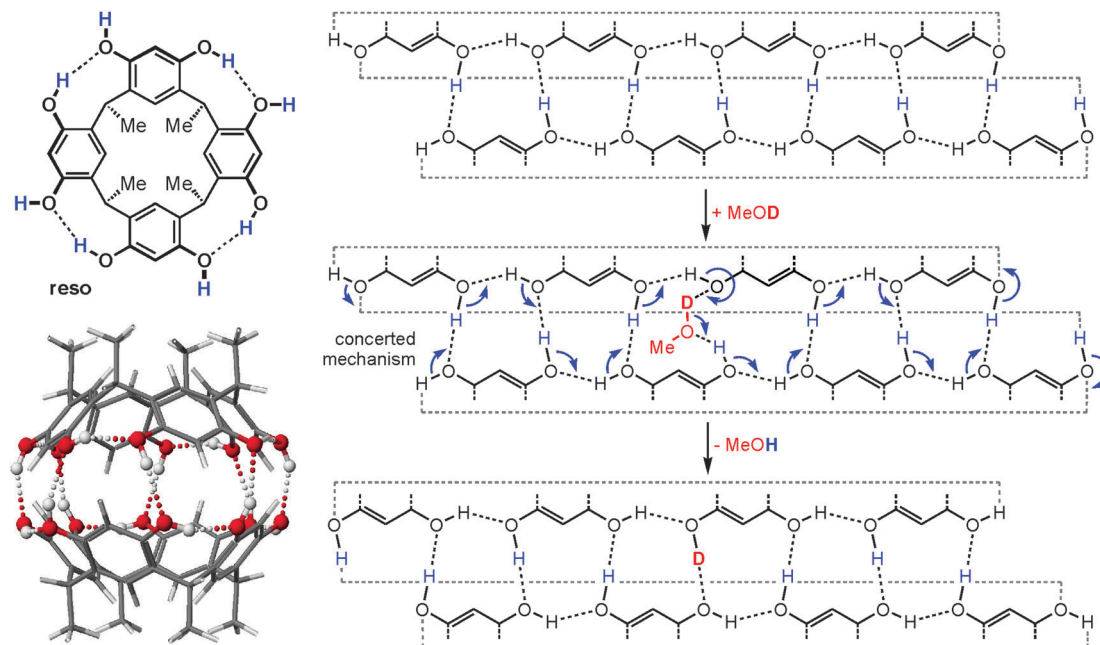
**Fig. 15** Left: chemical structure of the resorcinarene **reso** and force-field-optimized structure of the corresponding hydrogen bonded dimer. Right: mercator projection of the hydrogen bonding seam of the dimeric capsule and a concerted mechanism for the H/D-exchange reaction. Reproduced from ref. 62b with kind permission by the Royal Society of Chemistry.

in hydrogen bonding and form a seam of hydrogen bonds which meanders around the whole capsule. In marked contrast to expectation, a rather rapid exchange of all OH protons is instead observed, when the dimer is subjected to gas-phase HDX experiments with methanol-OD.[62] This surprising behaviour can be explained easily by invoking a concerted exchange mechanism as sketched in Fig. 15. Insertion of a MeOD molecule at any position of the hydrogen bonding opens the path for simple electron pair migrations around the whole seam. None of the OH protons needs to migrate. Energetically unfavourable charge separation intermediates, which would be the products of a proton shift from the capsule to the exchange reagent, can efficiently be avoided by such a mechanism, as the methanol-OD molecule serves simultaneously as a deuteron donor and proton acceptor. As all OH groups are held in position by the capsule scaffold, a concerted mechanism is feasible reminiscent of the well-known Grotthus-type proton migration in water.[63] In control experiments, resorcinarene dimers that are either tetramethylated or encapsulate guests that are too large to fit completely inside do not show such a fast exchange, because the hydrogen bonding seam is disrupted and no concerted mechanism possible.

## 5 Ion mobility spectrometry mass spectrometry

Since ion mobility instruments became commercially available, ion mobility spectrometry mass spectrometry (IMS-MS)[64] enjoys increasing popularity and has also been used to address structural questions in supramolecular chemistry.[65] Mass-selected ions are subjected into a drift cell, which is filled with a collision gas, often nitrogen, at pressures of a few millibars and are pulled at low velocities through the gas cloud. As the collisions are soft, fragmentation can usually be prevented. The larger the collision cross section of the ion under study, the more collisions it undergoes and the later it arrives at the detector. The arrival time can thus be used as a measure for the collision cross section and thus for the size of the ion. Collision cross sections can also be calculated theoretically quite precisely so that it is often possible to compare the theoretical values obtained for a series of different structures with the experimental values and decide, what the structure of the ion under study is – at least as long as the ions are not too floppy and are structurally well-defined.

A number of metallo-supramolecular containers has been investigated by ion mobility experiments. Stang and Bowers et al. applied it successfully to characterize rectangles, triangles, and the cage-like prism shown in Fig. 16.[66] In the arrival time distribution of the prism hexacation, three features are observed which can be assigned to the intact $M_6L_3^{6+}$ prism as well as $M_4L_2^{4+}$ and $M_2L^{2+}$ fragments which all have the same mass-to-charge ratio. Their assignment is supported by experiments in which the parent ions were collided with different collision voltages prior to the IMS experiments. The harsher the collision conditions, the more prominent the fragments are as expected. Furthermore, the calculated collision cross sections are in good agreement with the arrival times of the three complexes. Similarly, IMS experiments have been applied to giant metallo-supramolecular cube-like structures.[67]

Barran and Lusby et al. have applied IMS experiments to the trigonal prismatic cages $HL^1Pt$ and $L^2Pt$ depicted in Fig. 17.[68] Both cages can be synthesized as two different isomers depending on
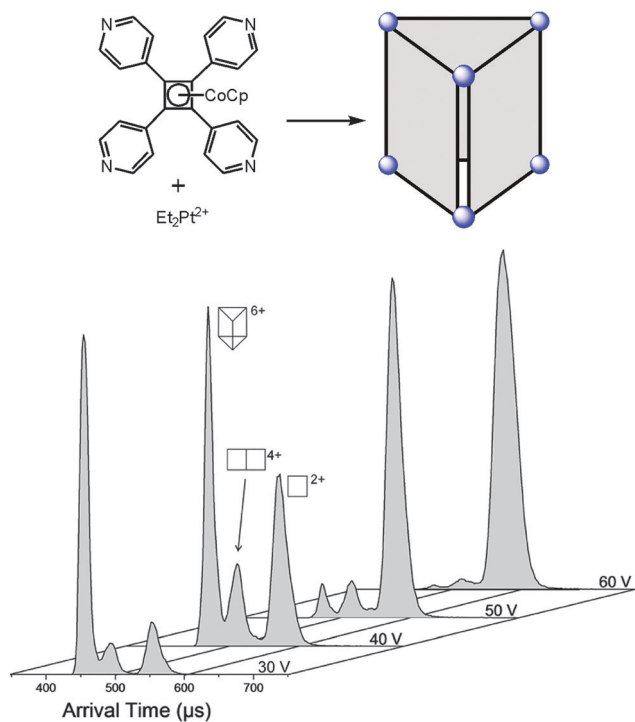
**Fig. 16** The $M_6L_3^{6+}$ prism (top) was subjected to IMS experiments. Clearly, several different complexes are observed which have the same $m/z$. Besides the intact prism hexacation, a quadruply charged $M_4L_2^{4+}$ and a doubly charged $M_2L^{2+}$ complex exist which can be separated by size in the drift tube. Experimental collision cross sections agree with calculated ones. The assignment is also secured by increasing collision voltages that provoke more and more fragmentation so that the intensity of the intact prism decreases in favour of more prominent fragment signals. It should be noted that the arrival time also depends on the charge state so that more highly charged ions travel faster through the drift cell. Adapted and reproduced from ref. 66 with kind permission by the American Chemical Society.



**Fig. 17** Top: chemical structures of the trigonal prismatic metallo supra-molecular cages $HL^1Pt$ and $L^2Pt$ in their cis- and trans-forms. Bottom: IMS experiments provide sufficient resolution to distinguish both isomers by their collision cross sections. Reproduced from ref. 68 with kind permission by the Royal Society of Chemistry.

the orientation of the bidentate, cyclometallated ligand at the metal centre, i.e. cis-$HL^1Pt$ versus trans-$HL^1Pt$ and cis-$L^2Pt$ versus trans-$L^2Pt$, and the question arises whether it is possible to distinguish the isomers by IMS.

For both cages, intact parent ions are successfully generated by electrospray ionisation through stripping off counterions. Fig. 17 shows the arrival time distributions for the $[M-3PF_6]^{3+}$ ions. Clearly, the IMS-MS experiments are capable of distinguishing the two isomers. The triply charged cis-$HL^1Pt$ complex was found to be smaller than the trans-$HL^1Pt$ cage with collision cross sections of 503 Å$^2$ and 572 Å$^2$, respectively. Even for the ($L^2Pt$) system, in which the two isomers only differ with respect of the relative positions of the pyridine versus phenyl ring of the bidentate ligand, the resolution of the IMS experiment is sufficiently high to separate the two isomers that have collision cross sections of 425 Å$^2$ and 479 Å$^2$.

# 6 Probing reactions of guest molecules inside containers

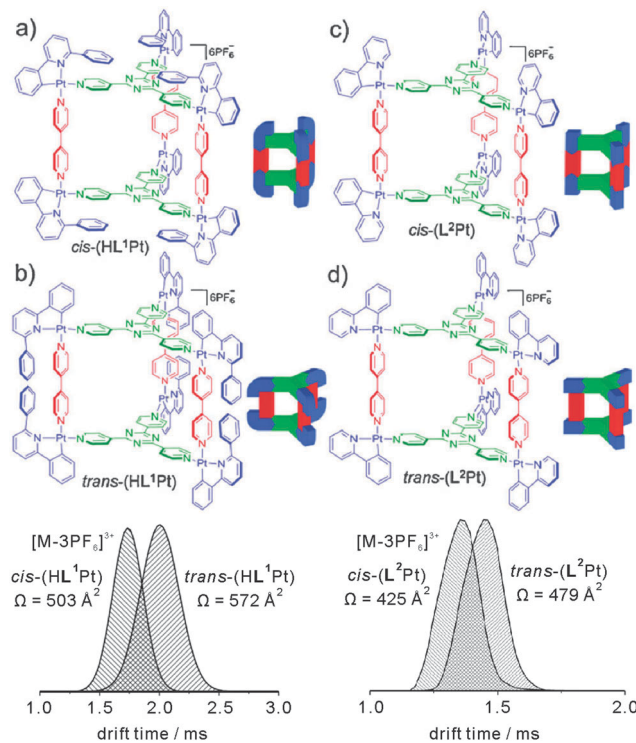The gas-phase studies on containers summarised above all addressed the container itself, its structure, its reactivity or its stability. Although guest molecules are present in many of the above examples, the studies above did not address the inner-phase reactivity – i.e. the reactivity of the guest inside the container and how it is affected by guest encapsulation. In a very recent study, Nau and Kalenius et al. used tandem mass spectrometry in concert with theory to investigate host–guest complexes of cucurbit[$n$]uril (**CBn**, $n$ = 6–8) containers with bicyclic azoalkanes **6**, **7** and **8** (Fig. 18).[69] Usually, electrospray ionisation of such cucurbituril host–guest complexes is readily achieved.[70] In the present case, protonation provides the necessary charge. The three cucurbiturils under study have different cavity volumes resulting in different guest selectivities. Nevertheless, they bind a range of differently sized bicyclic azoalkanes thus realizing different packing coefficients.[71]

In collision-induced dissociation experiments with mass-selected complex ions, the fragmentation patterns differ with respect to the size complementarity of host cavity and guest. Two reactions compete with each other: the dissociation of the guest from the complex and the cycloelimination of ethene followed by consecutive rearrangements and/or dissociation reactions of the product complexes formed in the retro-Diels–Alder reaction. The cycloelimination inside the cavity becomes dominant, when the packing coefficients are within a range of 30–50%. Smaller guest cations likely dissociate with a lower activation barrier as they can pass the inwards-bent seams of the cucurbiturils' carbonyl groups more easily. For larger guests, the cycloelimination of ethene, which is expected to have a
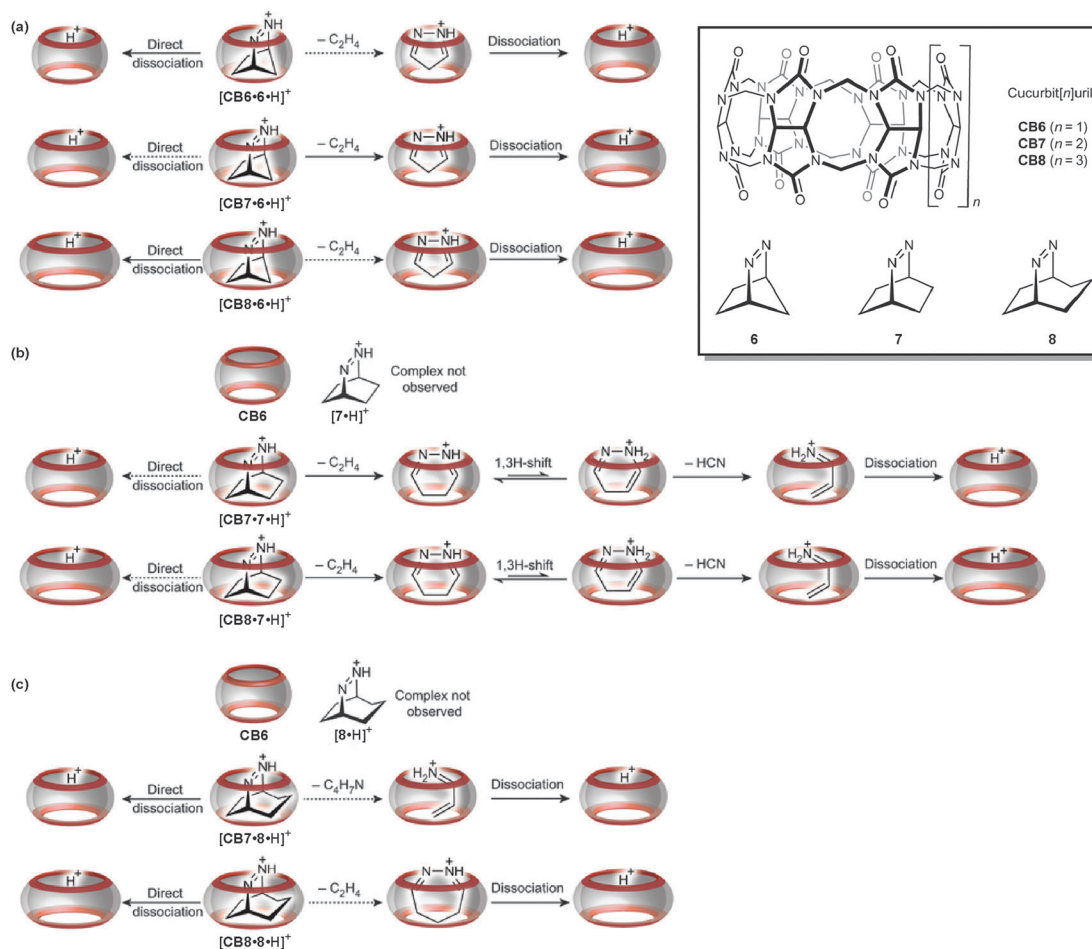
**528** | Chem. Soc. Rev., 2015, **44**, 515–531

This journal is © The Royal Society of Chemistry 2015

**Fig. 18** The gas-phase dissociation reactions of different cucurbituril–azoalkane complexes is characterised by a competition between complex dissociation and an inner-phase retro-Diels–Alder reaction. Depending on the size complementarity of the guest's van der Waals volume and the container cavity, reactivity significantly differs. Adapted and reproduced from ref. 69 with kind permission by the Nature Publishing Group.

positive activation volume, is probably hindered. A combination of constrictive binding and the void space inside the container thus emerges as important factors for the inner-phase reactivity.

# 7 Conclusions

In the present review, we have summarized the current status of how mass spectrometry contributes to the investigation of molecular containers, in particular to our understanding of metallo-supramolecular and hydrogen-bonded containers. The information delivered by mass spectrometry goes far beyond simply providing mass information and widens out knowledge of containers with respect to structural issues, the encapsulation of suitable guests, the stability of container guest complexes as well as their reactivity in solution and in the gas phase. Mass spectrometry is well suited to analyse rather complex mixtures so that self-assembly and self-sorting processes can be monitored. When it comes to the gas-phase chemistry of containers, many different aspects have been studied from the analysis of mechanistic aspects in cage contraction reactions through H/D-exchange processes in hydrogen-bonded capsules to the evaluation of inner-phase reactivity of the encapsulated guest inside the container.

The application of gas-phase chemistry to supramolecules is developing quickly. Mass spectrometry will thus also play a more and more important role in characterization of molecular containers. Certainly, many of the studies discussed above are far from economically useful applications and belong to the realm of fundamental science. Nevertheless, they underline how important the development and popularisation of novel methods such as ion mobility mass spectrometry are for the advancement of supramolecular chemistry.

## Acknowledgements

## Notes and references

1 (a) J. Rebek, Jr., *Chem. Soc. Rev.*, 1996, **25**, 255–264; (b) J. Rebek, Jr., *Acc. Chem. Res.*, 2009, **42**, 1660–1668.
2 (a) M. Yoshizawa, M. Tamura and M. Fujita, *Science*, 2006, **312**, 251–254; (b) M. D. Pluth, R. G. Bergman and K. N. Raymond,

This journal is © The Royal Society of Chemistry 2015

*Chem. Soc. Rev.*, 2015, **44**, 515–531 | 529

*Science*, 2007, **316**, 85–88; (*c*) T. S. Koblenz, J. Wassenaar and J. N. H. Reek, *Chem. Soc. Rev.*, 2008, **37**, 247–262; (*d*) A. Szumna, *Chem. Soc. Rev.*, 2010, **39**, 4274–4285; (*e*) Z. Dong, Q. Luo and J. Liu, *Chem. Soc. Rev.*, 2012, **41**, 7890–7908; (*f*) M. Raynal, P. Ballester, A. Vidal-Ferran and P. W. N. M. van Leeuwen, *Chem. Soc. Rev.*, 2014, **43**, 1734–1787; (*g*) B. Bibal, C. Mongin and D. M. Bassani, *Chem. Soc. Rev.*, 2014, **43**, 4179–4198.

3 R. Breslow and P. Campbell, *Bioorg. Chem.*, 1971, **1**, 140–156.

4 (*a*) P. Timmerman, W. Verboom and D. N. Reinhoudt, *Tetrahedron*, 1996, **52**, 2663–2704; (*b*) D. J. Cram and J. M. Cram, *Container Molecules and Their Guests*, Royal Society of Chemistry, Hertfordshire, 1997.

5 (*a*) K. Kim, N. Selvapalam, Y. H. Ko, K. M. Park, D. Kim and J. Kim, *Chem. Soc. Rev.*, 2007, **36**, 267–279; (*b*) J. Lagona, P. Mukhopadhyay, S. Chakrabarti and L. Isaacs, *Angew. Chem., Int. Ed.*, 2005, **44**, 4844–4870.

6 R. Warmuth and J. Yoon, *Acc. Chem. Res.*, 2001, **34**, 95–105.

7 (*a*) K. Hermann, M. Nakhla, J. Gallucci, E. Dalkilic, A. Dastan and J. D. Badjić, *Angew. Chem., Int. Ed.*, 2013, **52**, 11313–11316; (*b*) S. Kubik, *Chem. Soc. Rev.*, 2009, **38**, 585–605; (*c*) L. Cronin and A. Müller, *Chem. Soc. Rev.*, 2012, **41**, 7333–7334; (*d*) O. Bistri, B. Colasson and O. Reinaud, *Chem. Sci.*, 2012, **3**, 811–818; (*e*) B. M. Rambo, H.-Y. Gong, M. Oh and J. L. Sessler, *Acc. Chem. Res.*, 2012, **45**, 1390–1401.

8 (*a*) L. Adriaenssens and P. Ballester, *Chem. Soc. Rev.*, 2013, **42**, 3261–3277; (*b*) S. M. Biros and J. J. Rebek, *Chem. Soc. Rev.*, 2007, **36**, 93–104.

9 (*a*) P. D. Frischmann and M. J. MacLachlan, *Chem. Soc. Rev.*, 2013, **42**, 871–890; (*b*) S. J. Dalgarno, N. P. Power and J. L. Atwood, *Coord. Chem. Rev.*, 2008, **252**, 825–841.

10 Q.-F. Sun, J. Iwasa, D. Ogawa, Y. Ishido, S. Sato, T. Ozeki, Y. Sei, K. Yamaguchi and M. Fujita, *Science*, 2010, **328**, 1144–1147.

11 L. R. MacGillivray and J. L. Atwood, *Nature*, 1997, **389**, 469–472.

12 T. Gerkensmeier, W. Iwanek, C. Agena, R. Fröhlich, S. Kotila, C. Näther and J. Mattay, *Eur. J. Org. Chem.*, 1999, 2257–2262.

13 (*a*) J. Santamaría, T. Martín, G. Hilmersson, S. L. Craig and J. Rebek, Jr., *Proc. Natl. Acad. Sci. U. S. A.*, 1999, **96**, 8344–8347; (*b*) M. Yamanaka, A. Shivanyuk and J. Rebek, Jr., *J. Am. Chem. Soc.*, 2004, **126**, 2939–2943.

14 S. Rieth, K. Hermann, B.-Y. Wang and J. D. Badjic, *Chem. Soc. Rev.*, 2011, **40**, 1609–1622.

15 (*a*) C. A. Schalley, *Int. J. Mass Spectrom.*, 2000, **194**, 11–39; (*b*) C. A. Schalley, *Mass Spectrom. Rev.*, 2001, **20**, 253–309; (*c*) M. Vincenti and A. Irico, *Int. J. Mass Spectrom.*, 2002, **214**, 23–36; (*d*) B. Baytekin, H. T. Baytekin and C. A. Schalley, *Org. Biomol. Chem.*, 2006, **4**, 2825–2841; (*e*) Z. Qi and C. A. Schalley, *Supramol. Chem.*, 2010, **22**, 672–682; (*f*) F. Yang and D. V. Dearden, *Isr. J. Chem.*, 2011, **51**, 551–558; (*g*) L. Cera and C. A. Schalley, *Chem. Soc. Rev.*, 2014, **43**, 1800–1812.

16 F. W. McLafferty, *Science*, 1981, **214**, 280–287.

17 (*a*) G. Siuzdak, B. Bothner, M. Yeager, C. Brugidou, C. M. Fauquet, K. Hoey and C.-M. Change, *Chem. Biol.*,

1996, **3**, 45–48; (*b*) S. D. Fuerstenau, W. H. Benner, J. J. Thomas, C. Brugidou, B. Bothner and G. Siuzdak, *Angew. Chem., Int. Ed.*, 2001, **40**, 541–544.

18 M. W. H. Pinkse, C. S. Maier, J.-I. Kim, B.-H. Oh and A. J. R. Heck, *J. Mass Spectrom.*, 2003, **38**, 315–320.

19 W. Jiang, A. Schäfer, P. C. Mohr and C. A. Schalley, *J. Am. Chem. Soc.*, 2010, **132**, 2309–2320.

20 D. Gao, H. Liu, Y. Jiang and J. M. Lin, *Lab Chip*, 2013, **13**, 3309–3322.

21 D. Fabris, *Mass Spectrom. Rev.*, 2005, **24**, 30–54.

22 L. Konermann, J. Pan and Y.-H. Liu, *Chem. Soc. Rev.*, 2011, **40**, 1224–1234.

23 D. Schröder, *Acc. Chem. Res.*, 2012, **45**, 1521–1532.

24 See, for example: (*a*) S. Fürmeier and J. O. Metzger, *J. Am. Chem. Soc.*, 2004, **126**, 14485–14492; (*b*) C. Marquez and J. O. Metzger, *Chem. Commun.*, 2006, 1539–1541; (*c*) L. S. Santos and J. O. Metzger, *Angew. Chem., Int. Ed.*, 2006, **45**, 977–981; (*d*) J. Roithova, *Chem. Soc. Rev.*, 2012, **41**, 547–559; (*e*) J. Wassenaar, E. Jansen, Z.-J. van, F. M. Bickelhaupt, M. A. Siegler, A. L. Spek and J. N. H. Reek, *Nat. Chem.*, 2010, **2**, 417–421.

25 H. D. F. Winkler, E. V. Dzyuba and C. A. Schalley, *New J. Chem.*, 2011, **35**, 529–541.

26 (*a*) D. P. Weimann, H. D. F. Winkler, J. A. Falenski, B. Koksch and C. A. Schalley, *Nat. Chem.*, 2009, **1**, 573–577; (*b*) H. D. F. Winkler, D. P. Weimann, A. Springer and C. A. Schalley, *Angew. Chem., Int. Ed.*, 2009, **48**, 7246–7250; (*c*) Z. Qi, C. Schlaich and C. A. Schalley, *Chem. – Eur. J.*, 2013, **19**, 14867–14875; (*d*) H. D. F. Winkler, E. V. Dzyuba, A. Springer, L. Losensky and C. A. Schalley, *Chem. Sci.*, 2012, **3**, 1111–1120.

27 (*a*) S. Sakamoto, M. Fujita, K. Kim and K. Yamaguchi, *Tetrahedron*, 2000, **56**, 955–964; (*b*) K. Yamaguchi, *J. Mass Spectrom.*, 2003, **38**, 473–490.

28 J. S. Gardner, R. G. Harrison, J. D. Lamb and D. V. Dearden, *New J. Chem.*, 2006, **30**, 1276–1281.

29 O. D. Fox, J. Cookson, E. J. S. Wilkinson, M. G. B. Drew, E. J. MacLean, S. J. Teat and P. D. Beer, *J. Am. Chem. Soc.*, 2006, **128**, 6990–7002.

30 K. Suzuki, M. Tominaga, M. Kawano and M. Fujita, *Chem. Commun.*, 2009, 1638–1640.

31 M. Tominaga, K. Suzuki, M. Kawano, T. Kusukawa, T. Ozeki, S. Sakamoto, K. Yamaguchi and M. Fujita, *Angew. Chem., Int. Ed.*, 2004, **43**, 5621–5625.

32 M. Tominaga, K. Suzuki, T. Murase and M. Fujita, *J. Am. Chem. Soc.*, 2005, **127**, 11950–11951.

33 S. Sato, J. Iida, K. Suzuki, M. Kawano, T. Ozeki and M. Fujita, *Science*, 2006, **313**, 1273–1276.

34 C. Schmuck, *Angew. Chem., Int. Ed.*, 2007, **46**, 5830–5833.

35 W. Meng, B. Breiner, K. Rissanen, J. D. Thoburn, J. K. Clegg and J. R. Nitschke, *Angew. Chem., Int. Ed.*, 2011, **50**, 3479–3483.

36 S. P. Black, A. R. Stefankiewicz, M. M. J. Smulders, D. Sattler, C. A. Schalley, J. R. Nitschke and J. K. M. Sanders, *Angew. Chem., Int. Ed.*, 2013, **52**, 5749–5752.

37 P. Timmerman, K. A. Jolliffe, M. C. Calama, J.-L. Weidmann, L. J. Prins, F. Cardullo, B. H. M. Snellink-Ruël, R. H. Fokkens,

N. M. M. Nibbering, S. Shinkai and D. N. Reinhoudt, *Chem. – Eur. J.*, 2000, **6**, 4104–4115.

38 D. P. Weimann and C. A. Schalley, *Supramol. Chem.*, 2008, **20**, 117–128.

39 C. A. Schalley, J. M. Rivera, T. Martín, J. Santamaría, G. Siuzdak and J. Rebek, Jr., *Eur. J. Org. Chem.*, 1999, 1325–1331.

40 C. A. Schalley, T. Martin, U. Obst and J. Rebek, *J. Am. Chem. Soc.*, 1999, **121**, 2133–2138.

41 B. M. O'Leary, T. Szabo, N. Svenstrup, C. A. Schalley, A. Lützen, M. Schäfer and J. Rebek, Jr., *J. Am. Chem. Soc.*, 2001, **123**, 11519–11533.

42 A. Lützen, A. R. Renslo, C. A. Schalley, B. M. O'Leary and J. Rebek, Jr., *J. Am. Chem. Soc.*, 1999, **121**, 7455–7456.

43 C. A. Schalley, R. K. Castellano, M. S. Brody, D. M. Rudkevich, G. Siuzdak and J. Rebek, Jr., *J. Am. Chem. Soc.*, 1999, **121**, 4568–4579.

44 (a) M. Mäkinen, P. Vainiotalo, M. Nissinen and K. Rissanen, *J. Am. Soc. Mass Spectrom.*, 2003, **14**, 143–151; (b) H. Mansikkamäki, M. Nissinen, C. A. Schalley and K. Rissanen, *New J. Chem.*, 2003, **27**, 88–97; (c) H. Mansikkamäki, C. A. Schalley, M. Nissinen and K. Rissanen, *New J. Chem.*, 2005, **29**, 116–127.

45 (a) L. Avram and Y. Cohen, *J. Am. Chem. Soc.*, 2002, **124**, 15148–15149; (b) I. Philip and A. E. Kaifer, *J. Org. Chem.*, 2005, **70**, 1558–1564.

46 N. K. Beyeh, M. Kogej, A. Åhman, K. Rissanen and C. A. Schalley, *Angew. Chem., Int. Ed.*, 2006, **45**, 5214–5218.

47 B. H. Northrop, Y.-R. Zheng, K.-W. Chi and P. J. Stang, *Acc. Chem. Res.*, 2009, **42**, 1554–1563.

48 H. T. Baytekin, M. Sahre, A. Rang, M. Engeser, A. Schulz and C. A. Schalley, *Small*, 2008, **4**, 1823–1834.

49 Y.-R. Zheng and P. J. Stang, *J. Am. Chem. Soc.*, 2009, **131**, 3487–3489.

50 S. Sato, Y. Ishido and M. Fujita, *J. Am. Chem. Soc.*, 2009, **131**, 6064–6065.

51 Y. Rudzevich, V. Rudzevich, F. Klautzsch, C. A. Schalley and V. Böhmer, *Angew. Chem., Int. Ed.*, 2009, **48**, 3867–3871.

52 L. Cera and C. A. Schalley, *Chem. Soc. Rev.*, 2014, **43**, 1800–1812.

53 R. Zadmard, A. Kraft, T. Schrader and U. Linne, *Chem. – Eur. J.*, 2004, **10**, 4233–4239.

54 (a) J. Grunenberg and G. Barone, *RSC Adv.*, 2013, **3**, 4757–4762; (b) P. Ballester, *Chem. Soc. Rev.*, 2010, **39**, 3810–3830; (c) Z. R. Laughrey, T. G. Upton and B. C. Gibb, *Chem. Commun.*, 2006, 970–972. For a review, see: R. K. Castellano, *Curr. Org. Chem.*, 2004, **8**, 845–865.

55 S. S. Zhu, H. Staats, K. Brandhorst, J. Grunenberg, F. Gruppi, E. Dalcanale, A. Lützen, K. Rissanen and C. A. Schalley, *Angew. Chem., Int. Ed.*, 2008, **47**, 788–792.

56 C. A. Schalley, T. Müller, P. Linnartz, M. Witt, M. Schäfer and A. Lützen, *Chem. – Eur. J.*, 2002, **8**, 3538–3551.

57 B. Brusilowskij, S. Neubacher and C. A. Schalley, *Chem. Commun.*, 2009, 785–787.

58 (a) T. Wyttenbach and M. T. Bowers, *J. Am. Soc. Mass Spectrom.*, 1999, **10**, 9–14; (b) S. Campbell, M. T. Rodgers, E. M. Marzluff and J. L. Beauchamp, *J. Am. Chem. Soc.*, 1995, **117**, 12840–12854.

59 (a) E. Ventola, K. Rissanen and P. Vainiotalo, *Chem. – Eur. J.*, 2004, **10**, 6152–6162; (b) E. Ventola, A. Hyyryläinen and P. Vainiotalo, *Rapid Commun. Mass Spectrom.*, 2006, **20**, 1218–1224.

60 (a) E. Kalenius, D. Moiani, E. Dalcanale and P. Vainiotalo, *Chem. Commun.*, 2007, 3865–3867; (b) E. Kalenius, R. Neitola, M. Suman, E. Dalcanale and P. Vainiotalo, *J. Am. Soc. Mass Spectrom.*, 2010, **21**, 440–450.

61 (a) J.-P. Dutasta, *Top. Curr. Chem.*, 2004, **232**, 55–91; (b) A. Irico, M. Vincenti and E. Dalcanale, *Chem. – Eur. J.*, 2001, **7**, 2034–2042.

62 (a) M. Mäkinen, P. Vainiotalo and K. Rissanen, *J. Am. Soc. Mass Spectrom.*, 2002, **13**, 851–861; (b) H. D. F. Winkler, E. V. Dzyuba, J. A. W. Sklorz, N. K. Beyeh, K. Rissanen and C. A. Schalley, *Chem. Sci.*, 2011, **2**, 615–624.

63 C. A. Wraight, *Biochim. Biophys. Acta*, 2006, **1757**, 886–912.

64 T. Wyttenbach, P. R. Kemper and M. T. Bowers, *Int. J. Mass Spectrom.*, 2001, **212**, 13–23.

65 See, for example: (a) A. E. Counterman and D. E. Clemmer, *J. Phys. Chem. B*, 2001, **105**, 8092–8096; (b) R. R. Julian, R. Hodyss, B. Kinnear, M. F. Jarrold and J. L. Beauchamp, *J. Phys. Chem. B*, 2002, **106**, 1219–1228; (c) C. A. Schalley, J. Hoernschemeyer, X. Y. Li, G. Silva and P. Weis, *Int. J. Mass Spectrom.*, 2003, **228**, 373–388; (d) Y.-T. Chan, X. Li, M. Soler, J.-L. Wang, C. Wesdemiotis and G. R. Newkome, *J. Am. Chem. Soc.*, 2009, **131**, 16395–16397.

66 E. R. Brocker, S. E. Anderson, B. H. Northrop, P. J. Stang and M. T. Bowers, *J. Am. Chem. Soc.*, 2010, **132**, 13486–13494.

67 C. Wang, X.-Q. Hao, M. Wang, C. Guo, B. Xu, E. N. Tan, Y.-Y. Zhang, Y. Yu, Z.-Y. Li, H.-B. Yang, M.-P. Song and X. Li, *Chem. Sci.*, 2014, **5**, 1221–1226.

68 J. Ujma, M. De Cecco, O. Chepelin, H. Levene, C. Moffat, S. J. Pike, P. J. Lusby and P. E. Barran, *Chem. Commun.*, 2012, **48**, 4423–4425.

69 T.-C. Lee, E. Kalenius, A. I. Lazar, K. I. Assaf, N. Kuhnert, C. H. Grün, J. Jänis, O. A. Scherman and W. M. Nau, *Nat. Chem.*, 2013, **5**, 376–382.

70 See, for example: (a) W. Jiang, Q. Wang, I. Linder, F. Klautzsch and C. A. Schalley, *Chem. – Eur. J.*, 2011, **17**, 2344–2348; (b) J. Černochová, P. Branná, M. Rouchal, P. Kulhánek, I. Kuřitka and R. Vícha, *Chem. – Eur. J.*, 2012, **18**, 13633–13637; (c) J. P. Da Silva, N. Jayaraj, S. Jockusch, N. J. Turro and V. Ramamurthy, *Org. Lett.*, 2011, **13**, 2410–2413.

71 For a discussion of optimal packing coefficients, see: (a) S. Mecozzi and J. Rebek, Jr., *Chem. – Eur. J.*, 1998, **4**, 1016–1022; (b) S. Sánchez Carrera, J.-L. Kerdelhué, K. J. Langenwalter, N. Brown and R. Warmuth, *Eur. J. Org. Chem.*, 2005, 2239–2249; (c) R. Warmuth, J.-L. Kerdelhué, S. Sánchez Carrera, K. J. Langenwalter and N. Brown, *Angew. Chem., Int. Ed.*, 2002, **41**, 96–99.

This journal is © The Royal Society of Chemistry 2015

*Chem. Soc. Rev.*, 2015, **44**, 515–531 | 531